

**UNIVERSIDADE TÉCNICA DE LISBOA
INSTITUTO SUPERIOR TÉCNICO**

**MODELLING MACROALGAE IN
ESTUARIES**

**Trabalho Final de Curso
da Licenciatura em Engenharia do Ambiente**

Ana Rosa Rebelo Trancoso

n.º44769

Orientador

Prof. Ramiro Neves, D^{ep}to. de Eng.^aMecânica, IST

Co-Orientadores

Eng.º Pedro Pina, D^{ep}to. de Eng.^aMecânica, IST
Eng.º Luís Fernandes, D^{ep}to. de Eng.^aMecânica, IST

Lisboa, Novembro de 2002

ABSTRACT

In estuarine shallow waters, benthic flora can have a significant contribution to the total primary production. Attached macroalgae can be the prevailing primary producers in estuaries with small mean residence times, where phytoplankton does not reside long enough to uptake nutrients carried from upstream, and where vascular plants lack the needed support for root burying. The direct integration of water column properties by macroalgae growth processes makes them a local and reliable environmental indicator because they are instantaneously affected by high loads of nutrients, pollutants and sediments.

The aim of this work is the development of a benthic production model, integrated in a more general hydrodynamic and water quality model, MOHID. Focus has been given to light availability and interaction between macroalgae's processes and the water column / sediment interface. Like MOHID, the developed model uses an object-oriented programming philosophy, written in FORTRAN95 programming language. In addition, programming in Visual Basic for Applications was essential in data handling for result analysis.

In most estuarine systems, light has a preponderant role in macroalgae production rates. The results obtained suggest that macroalgae's productivity is highly sensitive to light extinction coefficients. Several light extinction formulations were tested with the conclusion that water column formulations must be preferentially based on local experimental relationships, which should include chlorophyll and particulate matter concentration effects on water column light penetration. Macroalgae's light limitation is controlled by the water column light extinction coefficient, which determines the amount of incident radiation in the weed bed. Nevertheless, the extinction occurring in the benthic bed is a determinant factor when they are dense or partially emerged.

The impact on the global nutrient dynamics of the estuary is local and not intense. However, macroalgae beds represent a large organic matter reservoir that increase diurnal oxygen gradients and can deeply affect the biogeochemical cycles of nutrient, carbon and oxygen when subject to extreme environmental conditions.

The developed model proved to be accurate in quantification of macroalgae biomass, and robust in the determination of macroalgae beds establishment sites. A more rigorous validation should be done, analysing seasonal variations in the weed bed, and its long term effect on water quality.

ACKNOWLEDGEMENTS

First of all, I am grateful to Professor Ramiro Neves for the opportunity of doing this work and for the knowledge transmitted at all times, during the past months.

I am also thankful to Master Pedro Pina who made this work possible through his interest and knowledge in this area and to Eng. Luís Fernandes, for his continuous support, as well as the dedication and patience he showed to have.

I am also indebted to Doctor Mark Baird, from the School of Mathematics of the University of New South Wales in Sydney, Australia, for his profitable suggestions, but specially, for the interest he showed from so far away in distance.

To the investigators and students working at MARETEC, I thank all for the stimulating working ambience provided. Special thanks must be given to Marcos Mateus and Susana Nunes for the Marine Biology concepts transmitted and to Paulo Chambel Leitão for his interested and critical perspective.

I also thank to my family for their unconditional support and for having always stimulated my interest in scientific and environmental matters. And to my mother, a unique thanks.

Finally, I thank to Rui for his interest and near support, as well as for the enrichment discussions we had.

INDEX

1	INTRODUCTION.....	1
1.1	PROBLEM DESCRIPTION	2
1.2	OBJECTIVE.....	3
1.3	FRAMEWORK	3
2	PRIMARY PRODUCTION.....	4
2.1	MACROALGAE	5
3	ECOLOGICAL MODELLING.....	7
3.1	GROWING AND FLOWING - MACROALGAE'S ESTABLISHMENT	8
3.1.1	<i>Erosion Zones</i>	8
3.1.2	<i>Deposition Zones</i>	9
3.2	ENVIRONMENT LIGHT AVAILABILITY	11
3.2.1	<i>Extinction of Light</i>	11
3.2.2	<i>Photosynthetic Response to Light</i>	14
3.3	MODEL IMPLEMENTATION	17
3.3.1	<i>Conceptual Model Scheme</i>	17
3.3.2	<i>Macroalgae Production Model</i>	20
3.3.2.1	Gross Growth	21
3.3.2.1.1	Temperature Limitation.....	22
3.3.2.1.2	Light Limitation.....	24
3.3.2.1.3	Nutrient Limitation	25
3.3.2.2	Respiration, Excretion and Mortality.....	26
4	METHODOLOGY	28
4.1	MOHID.....	28
4.2	BENTHIC MODEL.....	29
4.3	DATA HANDLING.....	29
5	RESULT ANALYSIS	30
5.1	REFERENCE RUN.....	31
5.2	LIGHT SENSITIVITY ANALYSIS	33
5.2.1	<i>Conclusion</i>	36
5.3	EFFECT ON DISSOLVED OXYGEN	37
5.4	MACROALGAE'S ESTABLISHMENT	38
6	CONCLUSIONS.....	42
7	FUTURE RESEARCH	43
8	REFERENCES.....	45

“Nature does nothing uselessly”

Aristotle

1 INTRODUCTION

Estuarine ecosystems are open and variable systems dominated and subsidized by many physical and biogeochemical processes. The complexity of their interactions and the magnitude of their consequences are still being recognized by the scientific community. Eutrophication phenomenon's frequently disrupt the delicate balance of the highly productive estuarine systems and are mainly due to excessive nutrient and sediment loads from river input, agricultural run-off and sewage disposal. Anthropogenic intervention is nowadays a constant issue so that an interdisciplinary approach is necessary for a sustainable aquatic resources management. Models that simulate hydrodynamic and major quality processes aid in developing hypotheses about the feedback mechanisms and allow water quality managers to predict the magnitude of the response to changes in management regimes.

The large existing gradients depend, mainly, on the degree of protection from direct oceanic forces, the quantity of freshwater input along with the amount of associated dissolved and suspended materials, and the depth of the estuary, resulting in large exchanges of biotic and abiotic materials, including water, salt, nutrients, sediments, and organisms with neighbouring systems. The exchange of organisms over millions of years has resulted in a rich heritage, and the biota is derived from marine, fresh-water, and terrestrial sources. Estuarine organisms have developed physiological and behavioural patterns to deal with the dynamic environment, and many are able to modify the physical environment. There is always a high diversity of physical habitats and the biota has fully exploited these different areas to make the biological habitat diversity even higher, placing estuarine ecosystems among the most productive natural systems of this planet (Mann, 1982)

The benthic system of the littoral zone is one of the most productive because it is where benthic photosynthesis is confined and in which the latter may exceed that achieved in the water column. Three categories of photosynthetic organism occur: (1) protists, essentially similar to those of phytoplankton but here associated with soft sediments, symbiotic within littoral animals such as reef coral, and occurring in various other microhabitats; (2) larger multicellular and macroscopic algae in a variety of forms that can range from the large leathery seaweeds of rocky outcrops and the finer to the more filamentous species growing on the surfaces of coarser seaweeds or on rock; (3) vascular plants in seagrass beds, mangrove swamps and salt-marshes.

The existence of three types of primary production units (phytoplankton, benthic algae and vascular plants) insure maximum utilization of light, profiting from the plenty supply of nutrients mixed by the water

movement due to tidal action. The countless trophic chains that can place on this basis and the consequently intense bacterial activity promote the rapid cycling of nutrients, rendering estuaries the unique capacity of self-depurating systems.

1.1 PROBLEM DESCRIPTION

Macroalgae, being immobile in the substratum, are reliable local indicators of water quality reflecting temporal changes and responding to different kinds of environmental stresses. These organisms directly integrate the water column properties being instantaneously affected by high loads of nutrients, pollutants and sediments.

Some macroalgae have an economic interest *per se* being used as agar and on food and cosmetic sectors. Algae can also cause taste and odour problems in water supplies, and filter clogging problems at water treatment facilities.

The human impact due to fishing activities, pollution and nutrient loads through sewage disposal or agricultural run-off can lead to algal blooms due to high nutrient loads. In addition, intertidal constructions (e.g. breakwater walls) and exhaustive dredging activities significantly reduce biodiversity, alter flow conditions and sediment dynamics promoting dispersion of opportunistic and epidemic algal species.

The integration of the biological benthic processes in a model that simulates hydrodynamics, sediment dynamics, pelagic biophysical processes and the biogeochemical cycles of the nitrogen, phosphorus and oxygen gives rise to a powerful tool that can be used in the planning of sustainable management of aquatic resources.

The inexistence of reliable data for the parameterization of benthic processes, especially for the smallest benthic organisms is mainly due to the difficulty of applying reliable and standardized sampling methods (Kröncke & Bergfeld, 2001). The simulation of these processes in artificial environments can offer the base knowledge for mathematical modelling, which then can be applied to reality, allowing a better understanding of the whole system.

1.2 OBJECTIVE

The purpose of this work is the development of a model that simulates benthic primary production, through the parameterization of the processes occurring at an estuarine level, focusing on the light availability and the interaction between nutrients in the water column, sediment dynamics and macroalgal growth. Coupled with a three dimensional hydrodynamic and water quality model, this work gives an initial frame for a more complete benthic ecological model.

1.3 FRAMEWORK

This work comprises three main chapters where sequential problem approach is made. The first chapter enlightens primary production effects on the total ecosystem, enhancing algae's importance in water quality modules. In the second chapter, a more in-depth discussion is made on the establishment of macroalgae erosion attachment zones, and on the characterization of the ambient light, being these aspects typically limitative or competitive advantageous in macroalgae's growth. The third part of this chapter is devoted to ecological modelling with a brief description about generic models, followed by the model hypothesis and formulations. Macroalgae production processes are described in the model implementation section, as well as the integration in MOHID conceptual scheme. The methodology followed in the accomplishment of this work can be found in chapter four and the result analysis in chapter five. Here, test runs are discussed and unfolded in a sensitivity analysis to the model and his application to Tagus Estuary. In the sixth chapter, conclusions are drawn from the work done and in chapter seven, future research themes are suggested.

*“Upon those who step into the same rivers,
different and different waters flow.”*

Heraclitus

2 PRIMARY PRODUCTION

The three primary production units of estuarine and coastal systems comprise microscopic planktonic organisms and micro and macroscopic benthic photoautotrophs.

In the pelagic system, **Phytoplankton** drifts in the water column and transport is the main influence in his behaviour, determining nutrient and light availability. Biomass production is mainly influenced by periodic phenomena like upwelling and thermoclines. In the benthic system, the **macroscopic algae**, although growing from the substratum are not rooted in it. Their holdfast system serves only as an anchorage to the bottom sediments. Like phytoplankton, their nutritive functions are solely dependent on the water column properties. **Vascular plants** (usually referred to as macrophytes) are rooted in the substratum and constitute several of the most productive coastal systems such as seagrass meadows, salt marshes and mangrove swamps¹. They colonize the upper intertidal areas where sediment deposition rates are considerable and water residence time is high enough to provide a good environment for root burying, as well as an unsteady substratum for epipellic algae's attachment. On the other hand, epiphytic filamentous algae can colonize vascular plants surface, with the competitive advantage of reducing light available for the plant. The attached **microphytobenthos** are associated with soft and mobile sediments where they can feed from the interstitial water and hide from predators or other environmental stresses by burying themselves. Forming a resistant biofilm, they colonize areas that appear to be too unstable for both macroalgae and plants, such as the high-energy sandy beaches and extensive adjacent sand flats (Mann, 1982).

In marine systems, the many species of phytoplankton may contribute 95% for the total primary production mainly due to the very large area of earth covered by the open sea. In shallow water near coasts and estuaries, attached single-celled algae (microphytobenthos), larger multicellular algae, and vascular plants make considerably more important contributions to the marine primary production due to the total amount of intertidal area. Phytoplankton represents approximately 62% in Ems-Hollard Estuary (The Netherlands) and only 42% in Occidental Scheldt (The Netherlands) (Nienhuis, 1992 in Portela, 1996). Mann (1972b) showed that in St.Margaret's Bay (Nova Scotia) which has an area of about 140 km², the macroscopic algae were contributing about 75% of the total primary production (in Mann, 1982).

¹ Seagrass meadows are distributed all over the globe wherever there is shallow water (except in high polar regions), but salt marsh and mangrove swamps replace each other geographically: salt marsh typify cooler and/or drier coasts while mangrove swamps hot and wet areas (Barnes & Hughes, 1988)

The existence of a benthic macroscopic bed of primary producers provides food and shelter to fish, invertebrates and larvae, promotes nutrient cycling and stabilizes flow conditions. This high total biomass and biodiversity promotes a high degree of ecosystem's self-organization leading to a rise in its carrying capacity.

2.1 MACROALGAE

Macroalgae have the advantage of being attached to a substratum while water flows through them, driven by tides, waves and wind. Any aquatic photosynthesizer rapidly builds up a gradient of carbon dioxide or nutrients in the boundary layer close to its surface. If the only method of obtaining carbon, nitrogen, etc., were by diffusion through these boundary layers, aquatic photosynthesis would be held to a very low level. However, the turbulence created by tidal and wind-driven currents moving over them while they remain in one place is an extremely effective mechanism for breaking down diffusion gradients (Mann, 1982; Hurd, 2000). That explains why, in those specific sites, the productivity per unit area of large attached algae can be an order of magnitude greater than that of phytoplankton (Mann, 1982).

Macroalgae can be the prevailing primary producers in small estuaries with low mean residence time whereas phytoplankton does not reside long enough to use the nutrients carried from the upstream rivers or discharges, and where sedimentation rates are low with two main important consequences: (1) more light available to the submerged macroalgae due to low water turbidity, and (2) the absence of soil does not support rooted macrophytes eliminating one strong competition relationship. This is the case of the north arm of Mondego Estuary where residence time is in the order of magnitude of one day and only the vegetable component not advected by water motion has conditions to grow. This is in contrast with the situation of the south arm characterized by low depths and water velocities, where the upstream part is almost silted up being, at present, mainly covered by *Spartina maritima* and *Zoostera noltii*, while in the downstream part, uncommon algal blooms (*Enteromorpha spp.*) have been observed due to the shallow waters, lower sedimentation rates and excessive nutrients release from the Pranto river into the estuary (Marques *et al.*, 1993; Martins *et al.*, 2001).

In Tagus Estuary, old oyster-beds provide the ideal substratum for macroalgae's attachment and, as so, the dominant species in this zones are, according to Ferreira (1989) *Fucus vesiculosus* L. (*Phaeophyta*), *Ulva lactuca* L. (*Chlorophyta*) and *Gracilaria verrucosa* (*Rhodophyta*), occupying a total area of 16 km² (12% of estuarine intertidal area) between 0.8 and 1.2 m above the hydrographic zero.

Summarizing, algae are important components of water quality models because:

- They are the basis of grazer aquatic food webs, and play an important role in detrital food webs, especially through the decay of macroscopic algae, the ones less grazed².
- Nutrient uptake during algal growth is the main process of nutrient removal from the water.
- Uptake of dissolved inorganic carbon (CO₂) during photosynthesis and its recycling during respiration can affect the water pH.
- Suspended algae are often a major component of turbidity.
- Photosynthetic oxygen production during daylight and consumption through respiration during the night can cause great diurnal variations in dissolved oxygen. When there are high loads of nutrients, the system will become over-saturated with biomass (algal blooms) producing oxygen and consuming nutrients during the day, supporting great populations of consumers and decomposers. By night, the oxygen is rapidly depleted creating anoxia conditions that disrupt the system resulting in massive fish kills under severe conditions. This phenomenon, usual in polluted coastal waters, is commonly addressed as **eutrophication**.

² Macroalgae and vascular plants are consumed by relatively few species, most notably by some sea-urchins and opisthobranch sea-hares.

*“Musical intervals may be expressed numerically.
Harmony of the universe may also be
expressed numerically.”
Pythagoras*

3 ECOLOGICAL MODELLING

Models vary in their structure and degree of complexity, and the selection of the type of model used depends on the information required by the modeller (Titus *et al.*, 1975 in Carr *et al.*, 1997). The factors influencing photosynthesis in aquatic plants and algae have been well described with mathematics or theoretical equations. However, empirical relations are unavoidable in productivity models, due to the complexity of the interaction of environmental factors influencing growth, respiration, washout, and decay.

A mechanistic approach was used in the modelling process, synthesizing the scientific information about the physiological processes involved in macroalgae growth and translating this understanding into mathematical terms. This kind of model allows the quantification of results and the typification of a broad range of environmental conditions. When the results divert from the natural behaviour of the system, they can reveal areas where future research is needed or even allow the statement of new hypotheses that can be tested with experimental work.

The work comprises three main issues that will be sequentially discussed. One is macroalgal establishment criteria where sediment dynamics and hydrodynamic processes are discussed in the macroalgal perspective. The second is the aquatic light environment, also influenced by sediment dynamics, but as the major limiting factor of macroalgae's growth. The third section comprises the ecological modelling formulations used as foundation of the developed model. These components cannot be considered alone because of their strong interaction and with the hydrodynamic conditions of the estuary.

3.1 GROWING AND FLOWING – MACROALGAE’S ESTABLISHMENT

Aquatic sessile organisms, such as macroalgae and colonial animals, risk being dislodged or broken by ambient water currents and waves. Yet they also depend on moving water for transport. Advection and diffusion transport are responsible for dispersing the spores or larvae, washing away waste products and sediments, and transport of dissolved materials such as nutrients and gases (Kaandorp & Kübler, 2001).

Benthic organisms usually encounter unidirectional currents or tidal currents that flow in one direction for several hours and then in the opposite direction. Attached organisms in intertidal water habitats are also exposed to waves. When water is passing in the substratum, a velocity gradient develops in the fluid between the surface of the substratum and the free stream flow (the boundary layer). Although a thin sub layer (mm’s thick) of laminar flow occurs along the substratum, water flow in the benthic boundary layer (m’s thick) is turbulent, so mass and momentum are mixed between the free stream flow and the bottom by swirling eddies (Kaandorp & Kübler, 2001). Thus, influenced by topography, the water flow encountered by a benthic attached organism can be quite different from the free stream flow over the site where it occurs.

In this boundary layer, macroalgae are subject to drag and lift perpendicular forces due to viscous resistance created by the water flow and to pressure difference across the body. Organisms in the accelerating flow in waves are also subjected to an accelerational reaction force (acting in the same direction as drag when water is speeding up, and in the opposite direction when water is slowing down).

Flexible organisms like macroalgae are pushed over by drag (and/or accelerational forces) and pulled back up by lift, which makes them flutter like a flag, increasing turbulent diffusion. This characteristic is one of the most important for macroalgal growth because without turbulent diffusion, uptake of nutrients and washing of excretion products (as oxygen) would be a mass-transfer limited process due to the low molecular diffusion across the diffusive boundary layer to macroalgae’s surface. The extent to which these hydrodynamic forces can be exerted without breaking macroalgae’s fronds depends on the stiffness and strength of the tissues, and the shape and size of the fronds (Kaandorp & Kübler, 2001).

3.1.1 Erosion Zones

In this work, benthic model interaction with the environment is conceptualized as fluxes of nutrients and organic matter from the bottom to the water column and vice versa, not specifying the morphological differences of macroalgal tissues (which are species characteristic). Nevertheless, the breakability effect is

accounted by the definition of macroalgal Erosion Zones. These are based on the concept of critical bottom shear stress, establishing an analogy with Partheniades's approach for sediment dynamics (Partheniades, 1965):

$$F_{ero} = \frac{dM_{ero}}{dt} = \begin{cases} E \left(\frac{\tau}{\tau_{ero}^*} - 1 \right) & \text{if } \tau > \tau_{ero}^* \\ 0 & \text{c.c.} \end{cases} \quad (3.1)$$

where F_{ero} is the erosion flux [$\text{kg}\cdot\text{m}^{-2}\cdot\text{s}^{-1}$], M_{ero} is the sediment eroded concentration [$\text{kg}\cdot\text{m}^{-2}$], t is time [s], E is the erosion constant [$\text{kg}\cdot\text{m}^{-2}\cdot\text{s}^{-1}$], τ is the bottom shear stress and τ_{ero}^* is the sediment critical erosion shear stress.

In this approach, when the bottom shear stress is higher than the critical value, erosion of sediments will occur. In a similar way, when the shear stress created on attached macroalgae by the water velocity is higher than a critical value, macroalgae will detach and, from this point, considered as particulate non-living matter.

The understanding of how marine macroalgae interact with their hydrodynamic microhabitat has increased substantially over the past 20 years, due to the application of tools such as flow visualization to aquatic vegetation, and *in situ* measurements of seawater velocity and turbulence (Hurd, 2000; Salomonsen *et al.*, 1999). According to Salomonsen *et al.* (1999), critical bottom shear velocities for macroalgal detachment can range from 0.012 (for small dimension macroalgae) to 0.15 $\text{m}\cdot\text{s}^{-1}$, i.e., from 0.14 to 22.5 $\text{N}\cdot\text{m}^{-2}$ in shear stress units.

3.1.2 Deposition Zones

Settlement is considered the most important stage in fouling organisms like macroalgae. Therefore, determination of macroalgae's attachment conditions constitutes a significant factor in macroalgal production patterns. Colonization of substrata involves adhesion of spores *via* the secretion of a glycoprotein adhesive, which in the settled spore forms a discrete gel-like pad on the surface (Finlay *et al.*, 2002). This explains why macroalgal spores settle gregariously justifying the weed bed modelling perspective (macroalgal processes are considered as water column-bottom fluxes and there is an inexhaustible pool of spores in the water column).

Sediments effectively compete with algal spores for space. Fine sediments will accumulate within the boundary layer of the substratum and fill up fine crevices and cracks. This will result in a less complex substratum, which will in turn reduce the probability of algal spore's attachment because they can be

easily washed away. Furthermore, smothering of algae by heavy sedimentation significantly reduces plant growth and survival because burial by sediments will increase deprivation of light and nutrients (Cheshire *et al.*, 1999; Airoldi & Cinelli, 1997).

In an estuarine system, Deposition Zones are spatially stable and have typical deposition patterns not just because of hydrodynamic factors but also due to salinity effects (Fernandes, 2001). Sediment dynamics is dependent on hydrodynamic factors (tidal flow and wave action), the nature of the substrate (topography and total sediment load) and salinity (flocculation effects). Hence, deposition fluxes can be given by:

$$F_{dep} = \frac{dM_{dep}}{dt} = \begin{cases} (CW_S)_B \left(1 - \frac{\tau}{\tau_{dep}^*} \right) & \text{if } \tau < \tau_{dep}^* \\ 0 & \text{c.c.} \end{cases} \quad (3.2)$$

where F_{dep} is the deposition flux [$\text{kg}\cdot\text{m}^{-2}\cdot\text{s}^{-1}$], M_{dep} is the sediment deposited concentration [$\text{kg}\cdot\text{m}^{-2}$], t is time [s], C is the near-bed sediment concentration [$\text{kg}\cdot\text{m}^{-3}$], W_S is the settling velocity [$\text{m}\cdot\text{s}^{-1}$], τ is the bottom shear stress and τ_{dep}^* is the sediment critical deposition shear stress (Krone, 1962). Typical estuarine sediment deposition fluxes are in the order of magnitude of approximately $5 \times 10^{-3} \text{ g}\cdot\text{m}^{-2}\cdot\text{s}^{-1}$ given by typical settling velocities of magnitude $10^{-4} \text{ m}\cdot\text{s}^{-1}$, near-bed sediment concentrations of $100 \text{ mg}\cdot\text{L}^{-1}$, and bottom shear stresses of about one half the critical deposition shear stress (τ_{dep}^*) (Dronkers & Leussen, 1988).

From this, one can see that macroalgal critical erosion shear stresses depends on the substratum they are attached to, and could be computed dynamically, varying with the amount of cohesive sediment deposited. However, for simplification and due to lack of in-depth research on this area, it was chosen not to dynamically simulate the critical detachment shear stress but rather use the sediment deposition flux and a critical shear stress for the lower and upper limit of the macroalgae's establishment areas.

Accumulation and mobilization of sediments depend also on the biological communities present in a number of ways: while turf algae can stabilize sediments by entrapment, the large and longer species can have sweeping movements that increase erosion fluxes to the water column. However, for the global sediment dynamics, macroalgal effects are in a much smaller scale than those caused by the hydrodynamic conditions and water column sediment loads.

3.2 ENVIRONMENT LIGHT AVAILABILITY

Photosynthetic organisms only exist where light is able to reach their cells. This means that phytoplankton is limited to the uppermost layers of the water column (photic zone) and that benthic algae are confined to shallow coastal waters where light reaches the bottom. The depth to which photosynthesis will occur is determined mainly by (1) the incident surface radiation, (2) the extinction of light in the water, and (3) the photosynthetic response to light.

Incident surface water radiation depends on factors such as clouds and dust in the atmosphere and solar elevation, the height of the sun above the horizon, which determines the angle at which the light strikes the surface of the water, and consequently, the amount of back-reflectance. Wind can also affect the incident intensity increasing the roughness of the water surface, which increases reflection of photons, especially at low solar altitudes. Shading from topographic features or riparian vegetation may also be significant factors.

3.2.1 Extinction of Light

Light attenuation through a column of water is one of the primary limiting variables in the growth of submerged flora, besides nutrients and temperature. Light availability can determine how much growth will take place but also which kind of species will develop. Vertical light attenuation and its spectral distribution are related to the absorption by water itself and the following additional components of the water column: photosynthetic biota, suspended particles and soluble compounds that may absorb and scatter the radiation beams. Although scattering does not remove photons from the water column, it is considered a light extinction phenomenon because it increases the photons mean path length and the probability of being absorbed by the absorbing components in the aquatic medium.

In the water column, the Lambert-Beer Law defines the attenuation of light with depth:

$$I(z) = I_0 e^{-kz} \quad (3.3)$$

where I [$\text{W}\cdot\text{m}^{-2}$] is the light intensity at a given depth z [m], I_0 is the light intensity at the surface and k the light extinction coefficient [m^{-1}].

The water column light extinction coefficient can be modelled statically for short-term simulations assuming a constant value for k , but for long-term simulations, it should be computed dynamically to account for the seasonal variations in water turbidity due to algal shading or variations in suspended solids

loads. For this reason, the light extinction coefficient is commonly defined as the linear sum of several partial extinction coefficients representing each component light absorption and/or scattering:

$$k = k_w + k_p + k_s + k_d \quad (3.4)$$

where k_w , k_p , k_s and k_d [m^{-1}] represent absorption and scattering of light energy due to water (w), phytoplankton (p), suspended particles other than phytoplankton (s) and dissolved organic matter, respectively (Parsons *et al.*, 1984).

The suspended particles include many different forms such as clay, particles, organic detritus, and organisms varying in size. Each of these extinction coefficients is highly dependent on wavelength. However, the use of an average extinction coefficient in the wavelength PAR³ rather than the value at particular wavelengths is the most practical (Parsons *et al.*, 1984).

The partial extinction coefficients can be determined from the specific extinction coefficient (specific absorptivity) and the concentration of the optically active components of the water column by the relation:

$$k_n = \kappa_n C_n \quad (3.5)$$

where k_n is the partial extinction coefficient of a particular component n, κ_n the specific extinction of that component and C_n the observed concentration (Christian, 1986).

The majority of the water quality models revised by Pina (2001) compute the water column light extinction coefficient considering phytoplankton self-shading effect and particulate suspended material, establishing the following relationship:

$$k = k_w + k_p C_p + k_s C_{ss} \quad (3.6)$$

where C_p is usually phytoplankton's chlorophyll concentration and C_{ss} is the total suspended solid concentration in the water column. The different set of parameters to be used should be based on local measurements (specially k_s) that allow the determination of the overall extinction coefficient.

By applying the Lambert-Beer law, with a given extinction coefficient, one can compute the light available for photosynthesis at a given depth.

The water-column light extinction is a determinant factor of macroalgae's growth because it limits intensity of incident radiation at the seaweed bed site but in the benthic boundary layer light will be extinct mainly

³ Photosynthetically active radiation (PAR) is the part of the visible spectrum that falls between 400 and 700 nm and it can be measured directly with a quantum sensor or estimated indirectly by assuming that PAR represents between 45 and 50% of total incident solar radiation (Carr *et al.*, 1997).

by macroalgal thalli⁴ that exert an intense self-shading effect. The total amount of shading effect depends of the thalli density, i.e., biomass density, as well as on their morphology. Macroalgae with apical growth will exert a less profound effect on light extinction than with diffuse growth, where cell divisions occur over the thallus as the whole organisms grows forming great opaque fronds. Apical macroalgae grow outward from the edges, or apices, having a less intensive shading effect, by light multiscattering effects.

Following this and recognizing that there are no sufficient in-depth studies of macroalgae's light needs, a somehow different approach must be undertaken for the light extinction coefficient in the benthic boundary layer. The prevailing light absorbing components will be macroalgae thalli and therefore the extinction coefficient must depend on their biomass, height and morphology. The joint dependence of these factors can be adjusted to the state variables of the model resulting in the following relationship:

$$k_{MA} = \frac{a_{abs} \times \Phi_{MA}}{\text{Min}(h_{MA}, h_{WC})} \times \text{Max}\left(\frac{h_{MA}}{h_{WC}}, 1\right) \quad (3.7)$$

where k_{MA} is the macroalgae bed light extinction coefficient [m^{-1}], a_{abs} is the carbon-specific shading area [$\text{m}^2\text{kgC}^{-1}$], Φ_{MA} is macroalgal biomass [$\text{kgC}\cdot\text{m}^{-2}$], h_{MA} is the macroalgal bed average height and h_{WC} is the water column height [m].

Increases in the carbon-specific shading area can be caused by frond growth and depend, as mentioned above, on thalli morphology. Macroalgae's carbon-specific absorption cross section values were determined by Enriquez *et al.* (1994) and vary between 11.1 and 145.3 $\text{m}^2\text{kgC}^{-1}$ (mean of 54.1 $\text{m}^2\text{kgC}^{-1}$) depending on the macroalgal morphology. The carbon-specific shading area accounts only for the surface area that causes shading, and thus, it will be lower. The definition of this parameter is also because macroalgae's efficiency in using incident light can be as low as 15% (Enriquez *et al.*, 1994).

When emerged, even if only partial, the self-shading effect is severely aggravated by the bending of the stipes and thus the multiplication by the second factor in equation (3.7) (see Figure 3.1).

⁴ Thalli – plural form of thallus

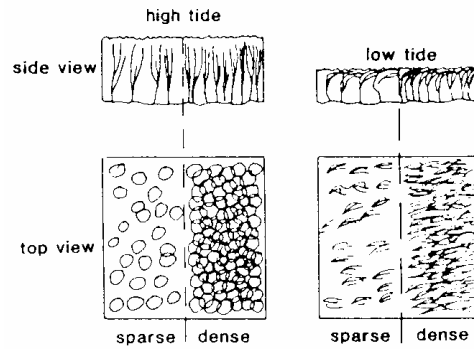


Figure 3.1 - Top and side views of sparse and dense macroalgae meadows at different tide levels. Side view shows vertical orientation, top view represents the area of overlap. After Denninson (1979) in Fonseca & Kenworthy (1987)

3.2.2 Photosynthetic Response to Light

When modelling the photosynthetic response to incident light one has to know that increases in light intensity lead to greater photosynthetic rates until some maximum is reached (optimal light intensity). At this point, producers cannot use more light since the enzymes involved in photosynthesis cannot act fast enough to process light quanta any faster. Therefore, rate of photosynthesis reaches an asymptote.

The relationship of photosynthetic rate to light intensity in macroalgae and seagrasses is similar to that found in single-celled algae and can be defined with Steele photoinhibition law (Steele, 1962):

$$\frac{P}{P_{\max}} = \frac{I}{I_{\text{opt}}} e^{(1-I/I_{\text{opt}})} \quad (3.8)$$

where P is the photosynthetic rate at a given light intensity I [$\text{W}\cdot\text{m}^{-2}$] for an organism that has a maximum photosynthetic rate P_{\max} at the optimal (saturating) light intensity I_{opt} . Evolution of photosynthetic rate with light intensity can be seen in Figure 3.2.

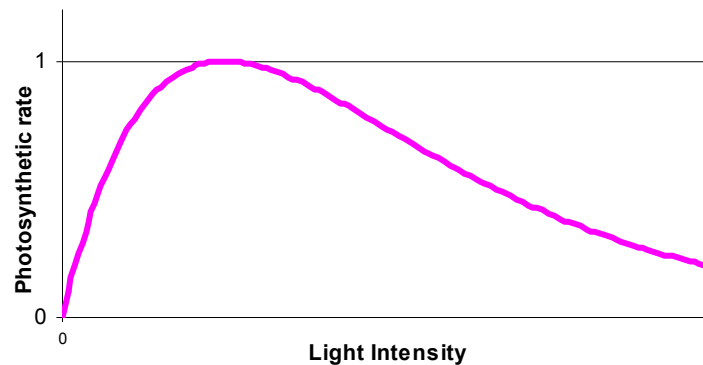


Figure 3.2 - Steele photoinhibition law

Surface environment light conditions can be quite different from those in the benthic boundary layer. The total light extinction in the water column limits the quality and intensity of incident radiation at the seaweed bed site, and thus, the photosynthetic response to available light.

As light enters the water column, the longer (red and infrared) waves are absorbed quite near the surface (principally by water absorption). Detrital particles and dissolved organic matter absorb most actively at shorter wavelengths, and phytoplankton absorbs light at two peaks corresponding to the action of chlorophyll. But in nature, each photosynthetic pigment (chlorophyll *a*, *b*, and *c*, fucoxanthin, peridin, etc.) has its own peculiar absorption patterns in the spectrum (Valiela, 1995). Macroalgae take advantage from this because, while phytoplankton is mainly composed by chlorophyll *a*, there are macroalgae with significant different arrays in photosynthetic pigments⁵. The green algae (*Chlorophyta*) absorb mainly in the red and blue wavelengths of the spectrum due to chlorophylls *a* and *b* as well as carotenoids such as xanthophylls and carotenes. Brown algae (*Phaeophyta*) contain chlorophyll *a* and *c*, as well as fucoxanthin pigments and use the green and yellow wavelengths more efficiently. Red algae (*Rhodophyta*) contain chlorophyll *a* and water soluble pigments in phycobiliproteins that allow absorption of light in the blue and green wavelengths (Valiela, 1995, Little & Kitching, 1996) enabling them to survive at greater depths, where these wavelengths still exist.

However, virtually all macroalgae are benthic and, therefore, inhabit a shaded environment. Thus, the efficiency of light collection is another fundamental aspect of their growth. Enriquez *et al.* (1994) empathizes the importance of the total quantity of pigments (magnitude of absorption) and thalli morphology in regulating algal growth at low light environments rather than their qualitative composition. The chromatic adaptation hypothesis is best applied in the explanation of macroalgae zonation patterns, associated with other physical and biological features such as desiccation tolerance, predation and competition, on rocky shores but not on the quantification of biomass (Little & Kitching, 1996)

The energy return per unit tissue produced (i.e. light absorption per unit plant weight) increases linearly with increasing pigment concentration (also per unit plant weight) but due to a pigments package effect associated with the complexity of multicellular tissues with increasing biomass, this efficiency in light absorption decreases with plant thickness (Enriquez *et al.*, 1994). However, macroalgal thallus morphology promotes multiscattering effects that increases total absorption in aquatic environments. Figure 3.3 shows how thallus structure acts as a fiber optic. Each photon of light is received by the plastids, which concentrate in the periphery of the utricles, which are inflated terminal regions of huge

⁵ All photosynthetic pigments with the exception of chlorophyll *a* (primary photosynthetic pigment) are known as accessory pigments. They comprise a pigment complex which acts to transfer light energy of a specific wavelength to chlorophyll *a* (Moon, 2001/2002)

cells, which lack cross walls (coenocytes). If a photon misses a plastid, it hits the highly structurally modified inner cell wall of the utricle and is reflected back into the utricle, either hitting one of the hundreds of plastids in the utricle, or being reflected back from the wall again (Moon, 2001/2002). This accounts for the photosynthetic density of macroalgae when compared to phytoplankton but this strategy represents a burden, limiting potential carbon turnover, mainly because the greater the photon absorption area, for the same biomass, the greater will be self-shading effects in the weed bed (see previous section), and thus, light limitation.

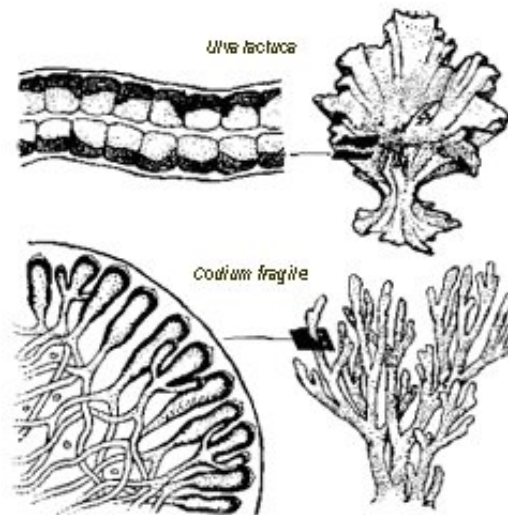


Figure 3.3 - Internal and external anatomies of *Ulva lactuca* and *Codium fragile*. After Abbot and Hollenberg (1976), Bold & Wynne (1985) and Ramus (1978) in Moon (2001/2002)

Inhibition by high light intensities is less marked in benthic flora than for single celled algae, probably because of self-shading within frond tissue (Valiela, 1995). This and the high light collection efficiency allow macroalgae optimal incident light intensities to be lower than the ones usually attributed to phytoplankton. Although literature reports a broad range of optimum values, Valiela (1995) averages a value of 90 W.m^{-2} while the optimum threshold for phytoplankton is 100 W.m^{-2} (Pina, 2001).

3.3 MODEL IMPLEMENTATION

New generation models tend to become much more biologically and chemically diversified than earlier models, as it is now largely recognized the need of an in-depth treatment of the full cycle of organic matter to truly simulate the ecosystem behaviour (Pina, 2001).

Two general approaches have been used to simulate algae in water quality models: (1) aggregating all algae into a single constituent (for example, total algae or chlorophyll *a*), or (2) aggregating the algae into a few dominant functional groups (for example, diatoms, dinoflagellates, benthic macro and microscopic algae, etc.). The first approach is commonly used in river models since the major focus is on short-term simulations (days to weeks) of water quality parameters such as dissolved oxygen, nutrients, and turbidity. Lake and reservoir models tend to be of the second approach since the focus is on long-term simulations (months to years) of eutrophication problems where seasonal variations are determinant (EPA, 1985).

In MOHID, the ecological model for the water column is based on the second approach, mainly adapted from EPA (1985) and pertains to the category of ecosystem simulation models, i.e., sets of conservation equations describing as adequately as possible the working and interrelationships of real ecosystem components. The ecological model has been developed for the computation of the sinks and sources terms of water properties transport equations (see **Section 4.1**) and these relevant terms are presented in appendix V. Such an approach is convenient to give these models the desired flexibility, providing it with the capacity of being coupled to either a Lagrangian or an Eulerian transport resolution method.

3.3.1 Conceptual Model Scheme

Ecological models usually differ on the organic matter pools described. In MOHID, living organic matter is sustained by three main compartments: (1) the primary producers with phytoplankton and macroalgae production models, (2) the consumers with micro and meso zooplankton and (3) the decomposers with simulation of bacterial growth. Bacteria are predated by microzooplankton (or ciliate) which can then be consumed, as well as phytoplankton, by the mesozooplankton. By applying grazing rates to the next trophic level not simulated, one can approximate the existing food webs in aquatic environments (**Figure 3.4**).

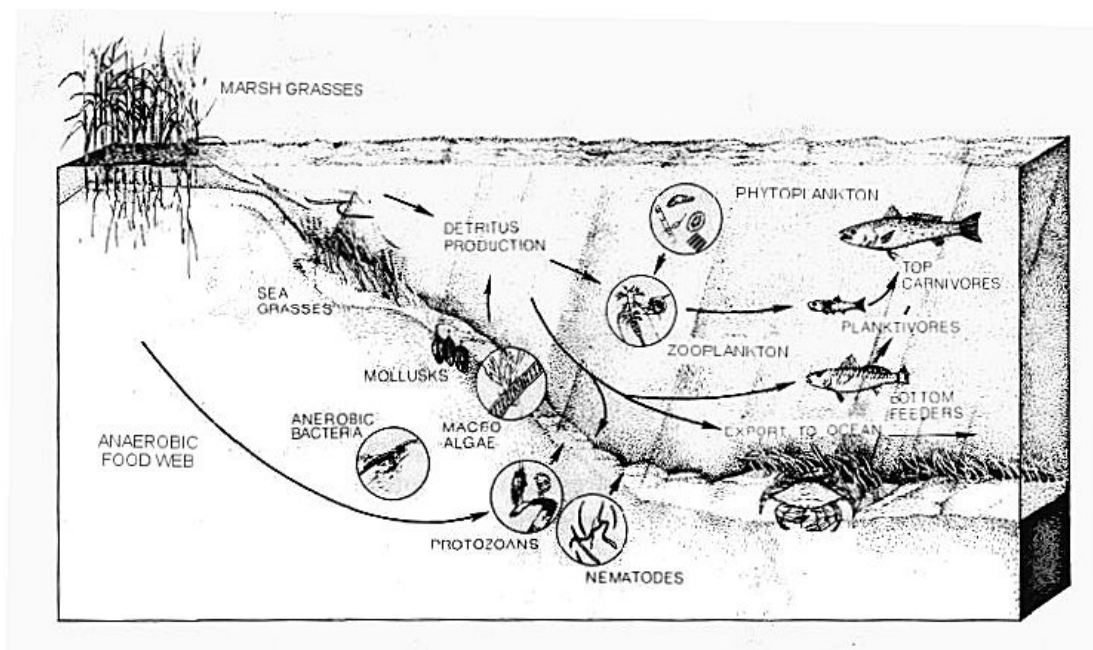


Figure 3.4 - Food web of a typical estuary showing some of the major trophic groupings

Dead organic matter can appear under the form of dissolved organic matter and suspended detritus or several pools of organic matter from highly refractory to highly labile. In MOHID, only Nitrogen and Phosphorous cycle are simulated explicitly and therefore, the simulation of organic matter assumes a constant C:N:P⁶ ratios (see section 3.3.2.1.3). Dead organic matter cycling appears in both cycles in particulate, dissolved organic refractory and non-refractory pools and the oxygen pool is also explicitly simulated.

MOHID is also prepared to run simulations with different degrees of complexity, reducing the costs in time and resources needed to obtain the desired results. For example, pelagic bacteria may not be explicitly simulated, appearing implicitly in the decay rate that is incorporated in the equations for organic matter compartments. This is what happens in the bottom sediments or in deep layer mineralization. The relevant processes are generally simulated by benthic organic matter degradation rates that influence nutrient and organic matter concentration in the pelagic phase. A conceptual model scheme can be visualised in Figure 3.3.

⁶ C – Carbon; N – Nitrogen, P - Phosphorous

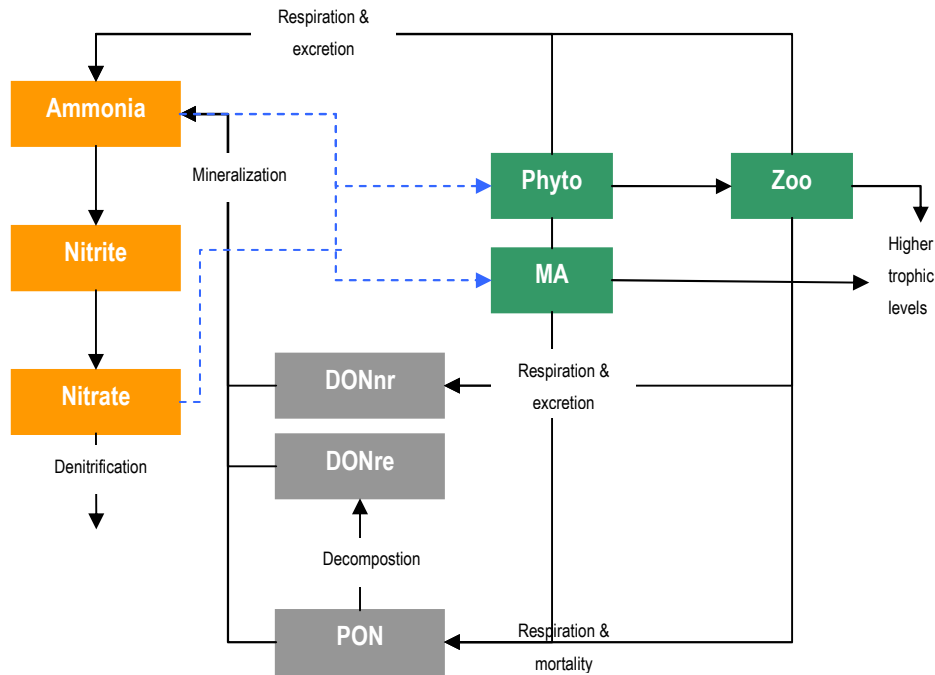


Figure 3.5 - Conceptual model scheme. After Pina (2001)

Phyo – phytoplankton; MA – macroalgae; Zoo – zooplankton; DONnr – non-refractory dissolved organic nitrogen; DONre – refractory dissolved organic nitrogen; PON – particulate organic nitrogen

Since macroalgae and phytoplankton have the same growth requirements (light and nutrients) and are subject to the same basic processes, the same formulations can be used, although the specific values of the coefficients will vary to characterize the difference between the two groups. The major differences can be summarized in:

1. Macroalgae are associated with the bottom substrate and are expressed in terms of areal densities [$\text{kg}\cdot\text{m}^{-2}$] rather than volumetric densities or concentrations.
2. Macroalgae are not subject to hydrodynamic transport.
3. Macroalgae have no settling losses, but instead they have additional losses by sloughing and scouring from the bottom substrate where bottom shear stress is high.
4. Macroalgae cannot firmly attach to the substrate in areas characterized by high sedimentation rates.
5. Emerged macroalgae are considered dormant, and the productivity yield after re-immersion is not affected (Bell, 1993).

One can consider an average height of weed bed because the more elongated are macroalgae's fronds, the more they will be subject to higher drag and friction forces, increasing the probability of being broken or detached from the substratum.

Thus, macroalgae production model brought new sinks and sources terms to the conservation laws of nutrients and oxygen that are summarily explained in appendix V and are based on the formulations presented in the next section.

3.3.2 Macroalgae Production Model

Following a mass-balance approach, for a bi-dimensional scalar property like macroalgae biomass, that is not advected nor diffused in the water velocity field, growth can be represented by equation (3.9)(see appendix IV).

$$\underbrace{\frac{\partial \Phi_{MA}}{\partial t} + \vec{v} \cdot (\nabla \Phi_{MA})}_{\frac{D\phi}{Dt}} = D \nabla^2 \Phi_{MA} + (F - P) \Leftrightarrow$$

$$\frac{\partial \Phi_{MA}}{\partial t} = (F - P) \quad (3.9)$$

where Φ_{MA} is the property concentration [kg.m^{-2}], t is the time [s], \vec{v} is the water velocity field [m.s^{-1}], D is the property diffusivity in the water [$\text{m}^2.\text{s}^{-1}$], and F and P are respectively sources and sinks of the property [$\text{kg.m}^{-2}.\text{s}^{-1}$].

Following an exponential population growth model, where the temporal variation of biomass depends on the existent biomass (Gotelli, 1995)), one can say that macroalgae dynamics are governed by the equation:

$$\frac{\partial \Phi_{MA}}{\partial t} = (\mu_{MA} - r_{MA} - ex_{MA} - m_{MA} - G_{MA}) \Phi_{MA} \quad (3.10)$$

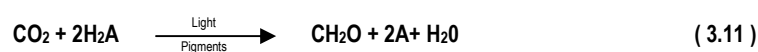
Where t is the time [day], Φ_{MA} macroalgae biomass [kgC.m^{-2}] and the others can be seen as the net production rate, composed of :

- μ_{MA} – macroalgae gross growth rate [day^{-1}]
- r_{MA} – macroalgae total respiration rate [day^{-1}]
- ex_{MA} – macroalgae excretion rate [day^{-1}]
- m_{MA} – macroalgae natural mortality rate (non-predatory) [day^{-1}]
- G_{MA} – grazing rate on macroalgae [day^{-1}] (see mortality in Section 3.3.2.2)

Equation (3.10) can be numerically solved in a number of ways (explicitly, implicitly, semi-implicitly, etc.). We choose to solve it explicitly because it shows fewer problems with mass conservation although it is less stable from a numeric point of view.

3.3.2.1 Gross Growth

Gross photosynthesis is the rate at which light energy is converted to chemical energy, transforming water and carbon dioxide into organic carbon and oxygen (Marker & Westlake, 1980 in Carr *et al.*, 1997). The basic photosynthetic equation can be expressed as:



This is a multistep process comprised of two independent series of reactions. The “light” reactions take place only when light is available and depend on the capture of photons by the photosynthetic pigments. In this process, an electron donor, H_2A , is split, liberating two electrons. In the case of oxygenic photosynthetic organisms (such as algae), the electron donor is water and two H_2O molecules are split to form an O_2 molecule and four protons, which will originate ATP and a strong reductant NADPH_2^7 , through a series of oxidation-reduction reactions (metabolic pathways). In the “dark” reactions, the ATP and NADPH_2 are used to reduce CO_2 into complex organic molecules (Valiela, 1995). This equation is very simplified because producers require a variety of inorganic nutrients, such as nitrate and phosphate, to provide the building blocks for the synthesis of the many compounds present in cells. The use of energy contained in organic compounds produced is a subject of section 3.3.2.2.

Macroalgal gross growth rate is a function of water temperature, availability of photosynthetically active radiation (PAR) and nutrients in the water column. The major growth limitation nutrients are nitrogen and phosphorous because carbon is often available in excess relative to nitrogen and phosphorous, and micronutrients like iron, manganese, etc. are only limitative in oligotrophic systems.

The most functional form of describing the joint dependence of the variables above is to define separate growth limiting factors, which can range from a value of 0 to 1. A value of 1 means the factor does not limit growth (i.e. light is at optimum intensity, nutrients are available in excess, etc.) The limiting factors are then combined with a maximum gross growth rate at a reference temperature in a number of ways. Four major approaches have been used to combine the limiting factors:

⁷ ATP – Adenosine 5'-triphosphate; NADPH_2 – Nicotinamide adenine dinucleotide phosphoric acid

- A multiplicative formulation in which all factors are multiplied together, assuming that several nutrients in short supply will more severely limit growth than a single nutrient in short supply. This can lead to excessively low growth rates when several nutrients are limiting. In addition, the severity of the reduction increases with the number of limiting nutrients considered in the model, making comparison between models difficult.
- A minimum formulation based on “Liebig’s Law of the Minimum” which states that the factor in shortest supply will control the growth of algae. This approach is often used only for nutrient limitation, with a multiplicative formulation for the light and temperature factor.
- A harmonic mean formulation based on an electrical analogy of several resistors in series:

$$\Psi(\text{Light}, \text{Nutrient}_1, \dots, \text{Nutrient}_n) = \frac{n}{\frac{1}{\Psi(\text{light})} + \frac{1}{\Psi(\text{Nutrient}_1)} + \dots + \frac{1}{\Psi(\text{Nutrient}_n)}} \quad (3.12)$$

This formulation includes some interaction between multiplied limiting factors, but it is not as severely limiting as the multiplicative formulation. This and the minimum formulation produce similar growth response curves under a wide range of conditions (Swartzman and Bentley, 1979 in EPA, 1985) but the first has the disadvantage of creating numerical errors in severe limiting conditions, by the division of very small numbers.

- An arithmetic mean formulation whose rationale is the same for the harmonic mean formulation. However, this formulation is rarely used because it does not restrict growth enough (it allows growths even if a critical nutrient such as nitrogen is totally absent, as long as other nutrients are available).

As so, the formulation adopted in MOHID is the multiplicative one, with the minimum formulation nutrients, resulting in:

$$\mu_{MA} = \mu_{\max}^{MA}(T_{ref}) \cdot \Psi(T) \cdot \Psi(I) \cdot \text{Min}(\Psi(N), \Psi(P)) \quad (3.13)$$

Where $\mu_{\max}^{MA}(T_{ref})$ is the maximum gross growth rate at the reference temperature [day⁻¹] and $\Psi(T)$, $\Psi(I)$, $\Psi(N)$ and $\Psi(P)$ are the temperature, light, nitrogen and phosphorous limiting factors, respectively.

3.3.2.1.1 Temperature Limitation

Although numerous temperature adjustment functions have been used to model algae, most of them fall into one of three categories: (1) linear increases in growth rate with temperature, (2) exponential increases in growth rate with temperature, and (3) temperature optimum curves in which the growth rate increases

up to a optimum and then decreases for higher temperatures. The first two approaches are best applied in situations where the water maximum temperatures are always below the organism's optimum because they increase indefinitely with temperature.

In MOHID, the concept of Thornton and Lessen (1978) is adopted to represent temperature limitation factor on autotrophic and heterotrophic organisms in temperate climate waters.

$$\Psi(T) = K_A(T) \cdot K_B(T) \quad (3.14)$$

$$K_A(T) = \frac{K_1 e^{\gamma_1(T-T_{\min})}}{1 + K_1 [e^{\gamma_1(T-T_{\min})} - 1]} \quad (3.15)$$

$$\gamma_1 = \frac{1}{(T_{\min}^{opt} - T_{\min})} \text{Ln} \left[\frac{K_2(1 - K_1)}{K_1(1 - K_2)} \right] \quad (3.16)$$

$$K_B(T) = \frac{K_4 e^{\gamma_2(T_{\max} - T)}}{1 + K_4 [e^{\gamma_2(T_{\max} - T)} - 1]} \quad (3.17)$$

$$\gamma_2 = \frac{1}{(T_{\max} - T_{\max}^{opt})} \text{Ln} \left[\frac{K_3(1 - K_4)}{K_4(1 - K_3)} \right] \quad (3.18)$$

In equations from (3.14) to (3.18), T_{\min}^{opt} and T_{\max}^{opt} are respectively the minimum and maximum temperature for the optimal growth interval [°C], and T_{\min} and T_{\max} are the minimum and the maximum tolerable temperature [°C] where processes are completely inhibited. The remaining constants (K_1 , K_2 , K_3 and K_4) control the shape of the temperature response curve. These values are assumed to be for all organisms in the model except for macroalgae. Figure 3.6 shows the variation of the temperature limitation factor with increasing temperature for phytoplankton and macroalgae.

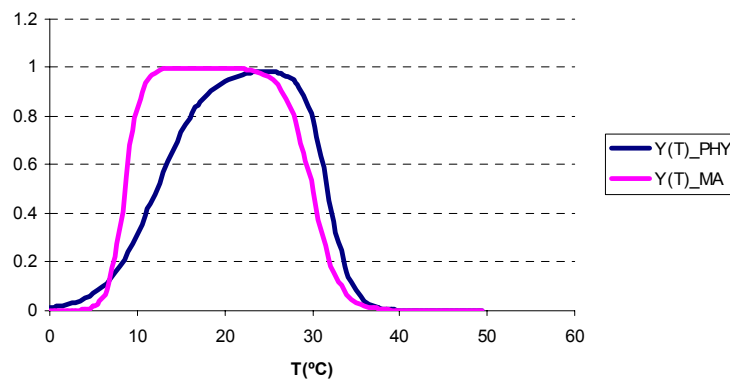


Figure 3.6 – Temperature limitation factor, $\Psi(T)$ with $K_1 = 0.05$, $K_2=0.98$, $K_3 = 0.98$, $K_4 = 0.02$ (Pina, 2001). For phytoplankton: $T_{\min}^{opt} = 25$, $T_{\max}^{opt} = 26.5$, $T_{\min} = 4$, $T_{\max} = 37$ (T °C). For macroalgae: $T_{\min}^{opt} = 12$, $T_{\max}^{opt} = 24$, $T_{\min} = 6$, $T_{\max} = 37$ (T °C) (Jones, 1993)

Several authors provide different ranges of temperature thresholds for macroalgae: Jones (1993) for *Codium fragile* L. (*Chlorofphyta*), Coffaro & Sfriso (1997) and Coffaro & Bocci (1997) for *Ulva rigida* L. (*Chlorofphyta*). The largest set was adopted, from Jones (1993) not only because it is consistent with the other two but also because we are not modelling one specific species of macroalga and other macroalgae species exhibit similar thresholds to *C. fragile*.

However, temperature has some influence in seasonal production cycles determining seasonal succession, for example, but there are few observations that demonstrate important effects of temperature on rates of primary production. Temperature may be more important as covariate with other factors than as an independent factor such as light and nutrients. For example, cells at low temperatures maintain greater concentrations of photosynthetic pigments, enzymes and carbon (see respiration in section 3.3.2.2) which results in a more efficient use of light (Valiela, 1995).

3.3.2.1.2 Light Limitation

The light limitation factor defines the relationship between ambient light levels and algal photosynthetic rate. According to section 3.2.2 the photosynthetic response to light is based on Steele's photoinhibition law. The relationship as expressed in equation (3.8) is usually used to fit experimental measurements of the effects of light on photosynthesis under laboratory conditions. In water quality models, these expressions are generally integrated over the depth of each model segment or layer since light varies with depth due to attenuation. Integrating Steele formulation in the benthic macroalgae bed height and assuming a classic Lambert-Beer function for the light extinction, the light limitation factor is:

$$\Psi(I) = \frac{\int_0^h P dz}{\int_0^h P_{\max} dz} = \frac{e^1}{k_{MA} \cdot h} \left[e^{-\frac{I_{oi}}{I_{opt}} e^{-k_{MA} \cdot h}} - e^{-\frac{I_{oi}}{I_{opt}}} \right] \quad (3.19)$$

with $h = \text{Min}(h_{MA}, h_{WC})$ and where I_{oi} is the incident radiation on macroalgae bed [$\text{W} \cdot \text{m}^{-2}$], I_{opt} the optimum light intensity for macroalgae photosynthesis [$\text{W} \cdot \text{m}^{-2}$], k_{MA} the light extinction coefficient in the macroalgae bed [m^{-1}], h_{MA} the average macroalgae bed height [m] and h_{WC} the water column height [m].

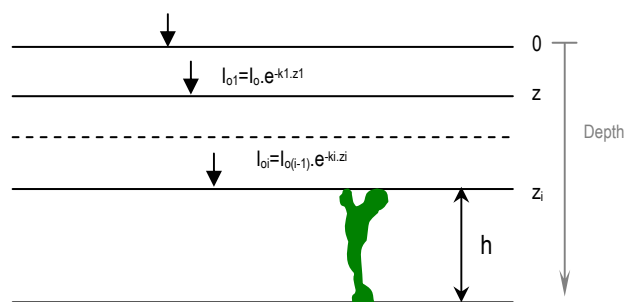


Figure 3.7 - Schematics of macroalgae light limitation factor algorithm

Incident radiation on the weed bed is obtained by sequential light extinction computations in each vertical water layer (Figure 3.7). The light intensity at the surface (direct and diffuse) is calculated in MOHID in the Surface Module.

3.3.2.1.3 Nutrient Limitation

The most common approach in computing nutrient limitation factors in algal models is based on Michaelis-Menten kinetics and assumes that the growth rates are determined by the external concentrations of available nutrients. External, here, refers to the nutrient concentration in the water column as opposed to the internal concentrations in the algal cells. This approach assumes that the nutrient composition of the algal cells remains constant (fixed stoichiometry models) and that growth and nutrient uptake rates are linearly dependent. Thus, macroalgae C:N:P ratio is 550:30:1 (atomic ratio) while for phytoplankton, zooplankton and non-living organic matter is assumed the Redfield ratio (106:16:1) (Atkinson & Smith, 1983; Falkowsky, 2000; and Baird *et al.*, 2001) The higher macroalgae ratio accounts for the amount of more structured carbon in the multicellular tissues than in single-celled algae. Although stoichiometric cellular ratios depend on species, cell dimension, external and physiological conditions, most water quality models use the fixed stoichiometry approach because it simplifies the model without prejudice of results, unless one wants to simulate explicitly luxury uptake and nutrient storage in organisms. This could be of interest in systems with seasonal variation of nutrient abundance, because the ability of macroalgae to store reserves gives them an advantage over phytoplankton as growth can take place immediately when photoperiod increases (e.g. late winter) (Valiela, 1995).

Under optimum temperature and light conditions, the limitation factor for nitrogen and phosphorous can be expressed as:

$$\Psi(N) = \frac{\Phi_{NH_4} + \Phi_{NO_3}}{K_N^{MA} + \Phi_{NH_4} + \Phi_{NO_3}} \quad (3.20)$$

$$\Psi(P) = \frac{\Phi_{IP}}{K_P^{MA} + \Phi_{IP}} \quad (3.21)$$

where Φ is the water column concentration in ammonia (NH_4^+), nitrate (NO_3^-) and inorganic phosphorous (IP) or orthophosphate (PO_4^{3-}), K_N^{MA} and K_P^{MA} are the nitrogen and phosphorous half-saturation constants, respectively. Ammonia, nitrate and K_N^{MA} are expressed in milligrams of nitrogen per litre while inorganic phosphorous and K_P^{MA} are in milligrams of phosphorus per litre.

With a high C:N:P ratio, the nutrient half-saturation constants for macroalgae are usually well above ambient nutrient concentrations, and hence, specific growth rates of these organisms are quite low as was already mentioned earlier (see parameters list in appendix VI).

3.3.2.2 Respiration, Excretion and Mortality

Biomass loss terms comprise respiration, excretion and mortality that are important components of nutrient recycling and represent the difference between gross and net growth. Respiration, excretion and gross growth rate should be modelled separately since respiration processes rates depend mostly on temperature while excretion and photosynthesis in the nutrient availability.

Total **respiration** can be defined as the sum of endogenous and photorespiration. The endogenous respiration is the process by which the energy contained in the organic compounds produced by photosynthesis is made available by a series of light-independent oxidative reactions⁸. Besides affecting the uptake rates of nutrient, temperature has a marked effect on dark reaction photosynthetic enzyme activity (Jones, 1993). Thus, the endogenous respiration can be described by the first term on the right side of equation (3.22).

In contrast to dark respiration, photorespiration in macrophytes is stimulated when light intensity and dissolved oxygen concentrations are high, typical of mid to late afternoon conditions on bright days (Carr

⁸ Respiration occurs in all organisms. In animals or many microbes, ingested or absorbed carbon compounds serve as the principal substrate for respiration. Organisms whose metabolism is based on organic compounds fixed by autotrophs are called heterotrophs. This is in contrast to autotrophs, defined as organisms able to use inorganic carbon (CO_2) by reductive assimilation to supply carbon requirements. Endogenous respiration is also referred to as dark or basal respiration.

et al., 1997). For this reason, total respiration can be computed with the second term of expression (3.23) (EPA, 1985).

Excretion can be formulated in a similar way as photorespiration, but depending directly of a light limitation factor because of high photosynthate and photorespiratory compounds excretion at both low light levels and inhibitory high light levels (EPA,1985) (equation (3.23)).

Mortality depends on grazing pressure, in one hand, and on physiological conditions of the cells on the other, and because of the higher organic matter turnover time when scaling up a trophic chain, they should be modelled separately, even when predators are not explicitly simulated. In this case, predatory rates can be assigned a constant value that reflects more or less the grazing intensity that macroalgae are subject to, in normal equilibrium conditions. Macroalgae's grazing rate should not be high because they are not preferential food items in the presence of phytoplankton. They have a higher C:N:P ratio and hence, have a low nutritive value for grazers.

Non-predatory mortality comprises senescence processes, stress due to severe nutrient deficiencies, extreme environmental conditions or toxic substances. It and can be modelled with a Michaelis-Menten formulation (EPA, 1985) to account for the effects of bacterial activity, assuming that bacterial activity increases in proportion to the algal densities at low biomass concentrations, but other factors limit decomposition rates at high algal densities. The dependence on gross growth rate reflects the physiological conditions of macroalgae's cells on algal decomposition.

Process	Units	Formulation	
Respiration	day ⁻¹	$r_e^{MA} = K_{re}^{MA} e^{0.069T} + K_{rp}^{MA} \mu_{MA}$	(3.22)
Excretion	day ⁻¹	$ex_{MA} = K_e^{MA} \cdot \mu_{MA} \cdot (1 - \Psi(I))$	(3.23)
Non –predatory mortality	day ⁻¹	$m_{MA} = m_{\max}^{MA} (T_{ref}) \frac{\frac{\Phi_{MA}}{\mu_{MA}}}{K_m^{MA} + \frac{\Phi_{MA}}{\mu_{MA}}}$	(3.24)

Table 3.1 - Respiration, excretion and non-predatory mortality formulations

where T is temperature [°C]; K_{re}^{MA} the endogenous respiration constant [day⁻¹]; K_{rp}^{MA} is the fraction of actual photosynthesis rate which is oxidized by photorespiration [adim]; K_e^{MA} is the fraction of photosynthesis excreted [adim]; $\Psi(I)$ is the light limitation factor (section 3.3.2.1.2) [adim]; $m_{\max}^{MA} (T_{ref})$ the maximum non-predatory mortality rate at reference temperature [day⁻¹]; Φ_{MA} the macroalgae concentration [kg.m⁻²] and K_m^{MA} the half-saturation constant for macroalgal non-predatory mortality [kg.m⁻².day⁻¹].

“The simplest solution is often the correct one.”

Occham's Razor

4 METHODOLOGY

The developed model is based on several parameterizations of biological and physiological process simulating macroalgae's growth and the environmental factors that influence photosynthesis, respiration, washout and decay of these organisms, allowing the dynamical study of the system and describing production over a day, a season or even several years.

The developed model is incorporated in the three-dimensional free surface water modelling system MOHID. Like MOHID, the developed model uses an object-oriented programming philosophy, written in FORTRAN95 programming language. Investigators under the direction of Prof. Ramiro Neves (MARETEC) have developed MOHID and its sphere of action comprises hydrodynamics, transport phenomena, sediment dynamics and water quality studies in several estuaries. The layered approach of the object-oriented philosophy allows an easy addition of new modules facilitating the integration of new processes.

4.1 MOHID

Following an object-oriented programming philosophy, in MOHID there can be identified many classes⁹ which are responsible for the flow properties (Hydrodynamic, Turbulence modules), for the pelagic system processes (Water Properties, Advection-diffusion and Water Quality), for the benthic processes (Sediment Properties, Consolidation and Bottom), and for the grid of the model (Bathymetry, Geometry). The pelagic system processes comprise the transport of the water column properties (e.g., salinity, temperature, sediments, nutrients, phytoplankton, etc.) interacting with the module Bottom, that is mainly responsible for the computation of erosion and deposition phenomena. An overview of the model's structure can be found in Miranda *et al.*, 2000.

This work has profited from the current re-structuration of MOHID that describes sediment, water column and their interface processes in three different modules. The interface module (BOTTOM), can exchange information with the other compartments establishing unidirectional client/server relationships as a client of the Water Properties module. The benthic model will be a class of the module BOTTOM because it depends on the water column for the nutrient cycle and on the sediment dynamics for the establishment of macroalgae's growth areas.

⁹ An object is an instance of a class and a module is comprised of one or more classes. A class has attributes that are values when applied to an object.

A brief description of MOHID basic hydrodynamic processes can be seen in appendix III. For transport equations of properties see appendix IV and for their sinks and sources terms see appendix V.

4.2 BENTHIC MODEL

The benthic model development methodology followed was comprised of two main parts. The first part consisted in the necessary bibliographic research and understanding MOHID structure and coding style, so that the benthic model could be written on a comprehensive basis, for all past, present and future users and developers of MOHID. The benthic model was prepared not only for the simulation of macroalgae processes but also for other organisms processes such as microphytobenthos or filter feeders, by the merely addition of formulations and parameters. All code was organized in a way that lessens the difficulty of these future implementations.

The second part, on the parameterization of the ecological processes, was inspired on other ecological models and studies for macroalgae and/or macrophytes growth, namely CSIRO Simple Estuarine Response Model (Baird *et al.*, 2001), Computational Aquatic Ecosystem Dynamic Model (CAEDYM) (Hamilton & Herzfeld) and EPA proposed model (EPA, 1985).

4.3 DATA HANDLING

Programming in Visual Basic for Applications (VBA) language was an essential part of this work because the macros developed lessen the difficulty of treating the large amount of data produced by MOHID making result analysis a more expeditious process. These macros are available to all other users of MOHID.

The usage of a Graphical Interface was of indubitable help in strategizing the data input and in visualizing the output data (see appendix II).

5 RESULT ANALYSIS

For the sensitivity analysis, several simulations were made in a schematic estuary (Figure 5.1), with a M2 tide imposed¹⁰. Analysed results were based on average values given by time series on the boxes and points defined. Due to the importance of light environment for photosynthetic organisms (Section 3.2), several two-day runs were made with different light extinction coefficient in the water column (k_{WC}), with different shading areas for macroalgae, with different initial biomass values, and for winter and summer days. All other parameters were maintained constant (list in appendix VI).

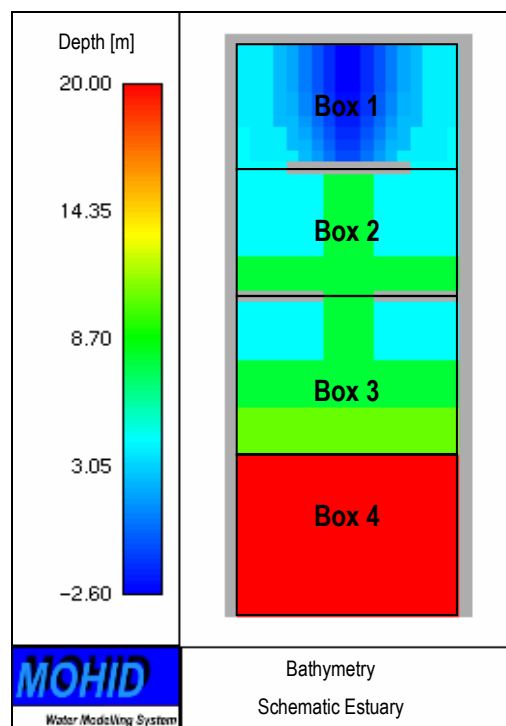


Figure 5.1 – Bathymetry (walls are in grey colour and the ocean boundary is in the bottom face of box 4)

¹⁰ This means that the amplitude is constant, only simulating high and low tide, neglecting spring and neap tide amplitude variations. This term alone would give the tide if the sun could be neglected, and if the moon orbited in a perfect circle in the plane of the earth's equator (Phillips, 1999)

5.1 REFERENCE RUN

The reference run comprises the following studied values:

Parameter	Value
k_{WC}	$k_{WC} = 0.08 + 0.11 * C [mgChla.m^{-3}]$ (Rivera, 1997)
a_{abs}	$5 m^2kgC^{-1}$
Φ_{MA}^0	$0.05 kg/m^2$
Φ_{phy}^0	$1 mg/L$
Time	From 2000/01/01 to 2000/01/03

Table 5.1 – Reference Run

As expected, macroalgae grow in the intertidal zone and not in the deepest zone of the estuary, near the oceanic boundary (Figure 5.2a). In this figure, box 2 and box 3 series are underneath box 4 series. There is no temperature limitation because temperature is approximately 18°C (Figure 3.6) and there is no nutrient limitation (limitation factor near 1) as showed in Figure 5.2c. The growth limitation observed in all boxes except box 1 is mainly due to complete light limitation below 4 m depth (Figure 5.2b). Thus, the result analysis will be focused in box 1, which comprises the intertidal zone with depths between -2.6 and 4 m.

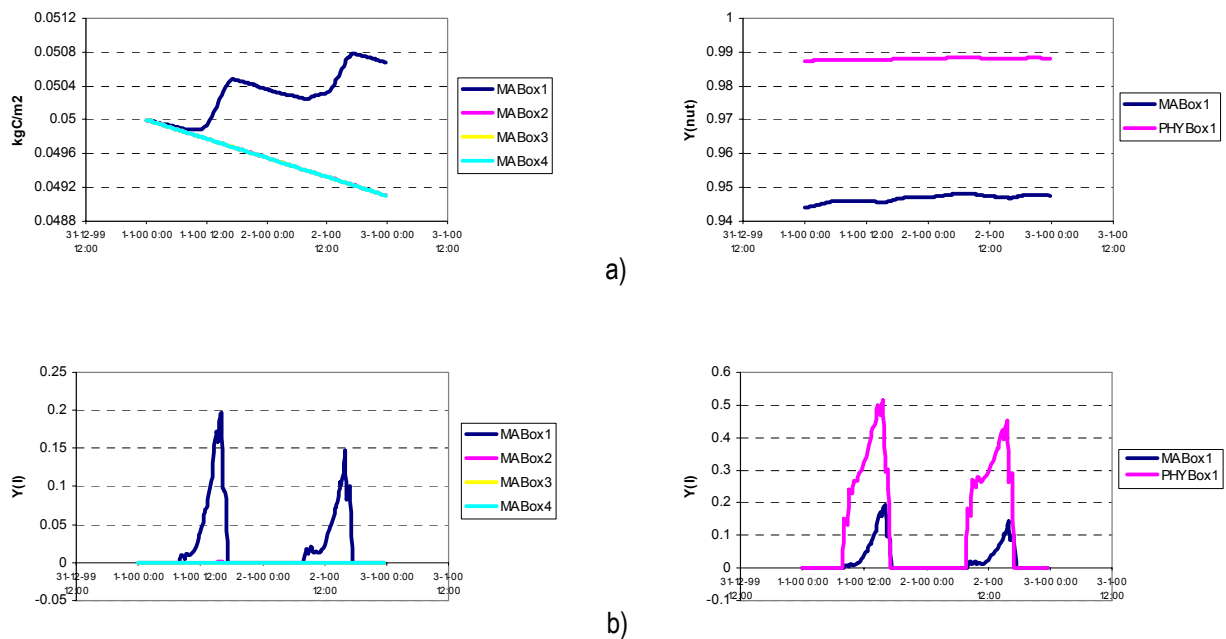


Figure 5.2 - Macroalgae and phytoplankton growth limiting factors (reference run - winter): a) macroalgae biomass; b) macroalgae light limiting factor c) macroalgae and phytoplankton nutrient limiting factor integrated in box 1; d) macroalgae and phytoplankton light limiting factor integrated in box 1

In box 1, daylight period is between 8:00 and 17:20, and macroalgae light limitation factor reaches its maximum at 16:00 in both days. This factor increases slower than it decreases, and slower than phytoplankton light limitation factor, because it has a linearly dependence with macroalgae's biomass. This is also the reason for the lower limitation factor values in the second day and it is in agreement with the postulated fact that macroalgae have lower availability of light in more dense weed beds. Phytoplankton's growth is also causing lower incident radiation intensities in the weed bed. Light and nutrient limitation factors are always higher for phytoplankton than for macroalgae, but differences are in the magnitude 0.3 and 0.04, respectively, indicating that light is also the limitation factor for these organisms.

Since light is the determinant variable, the reference simulation in summer (from 2000/06/01 to 2000/06/3) resulted in naturally higher biomass values, because of high radiation intensity, but in similar biomass evolutions (upper left corner of Figure 5.3). As the photoperiod is larger (from 5:20 to 20:00), light limitation factor are also higher than in winter in the first and last parts of the day. In the early afternoon, photoinhibition leads to lower light limitation factors in summer, but the total biomass production is higher than in winter.

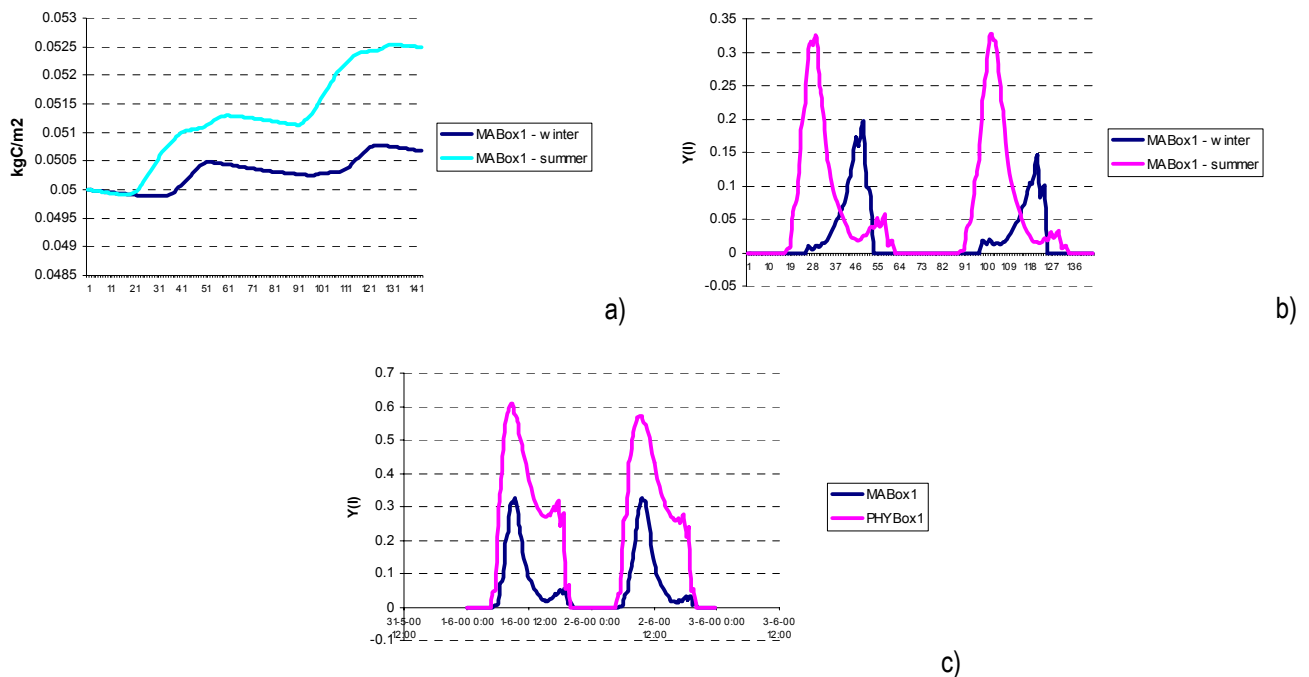


Figure 5.3 - Reference Run – Summer: a) macroalgae biomass in winter and summer runs, in box1; b) macroalgae light limiting factor in winter and summer runs, in box 1; c) macroalgae and phytoplankton light limiting factor in the summer run, in box 1.

5.2 LIGHT SENSITIVITY ANALYSIS

Several simulations were made with different water column light extinction coefficient (k_{WC}) and compared to the reference run (for the simulation in winter). The different formulations used are presented in Table 5.2 and Figure 5.4.

Run	Formulation	Study site	Literature
Ref	$k_{WC} = 0.08 + 0.11Chla$	Cape Bolinao, Philippines	Rivera (1997)
A	$k_{WC} = 0.08 \text{ m}^{-1}$	-	-
B	$k_{WC} = 0.04 + 0.0088Chla$	Ocean	Parsons <i>et al.</i> (1984)
C	$k_{WC} = 0.16 + 0.019Chla$	Mediterranean sea	Arhonditsis <i>et al.</i> , 2000
D	$k_{WC} = 0.08 + 0.11Chla + 0.036C_{ss}$	Tagus Estuary	Pina, 2001

Table 5.2 - Studied light extinction coefficient formulations; Chla is chlorophyll concentration [$\text{mgChla}\cdot\text{m}^{-3}$] and C_{ss} is total suspended particulate material [mgL^{-1}]

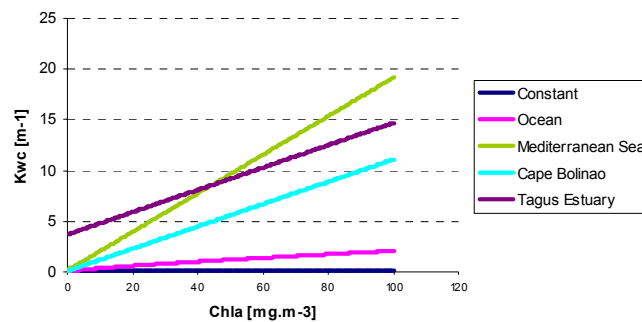


Figure 5.4 - Water column light extinction formulations [$C_{ss} = 100 \text{ mg}\cdot\text{L}^{-1}$]

Considering a constant water column light extinction coefficient ($k_{WC} = 0.08 \text{ m}^{-1}$) maximum biomass increases 20.4 %, almost 20 times more than the reference run in box 1 (1.4%) and there is a positive net growth in all the boxes (Figure 5.5a). Photoinhibition occurs for all boxes (except in box 4) and macroalgal nutrient availability is much more pronounced during the photoperiod but is not enough to be considered a severe limitation (minimum value of 0.98). This is also due to the large increase in phytoplankton biomass and to the fact that phytoplankton shading effect is not accounted by the k_{WC} , thus, macroalgae growth is more affected by phytoplankton in the nutrient availability than in light availability. It is clear that the k_{WC} used is excessively low because, in estuaries, it is not frequent to have light penetration depths higher than 8 meters.

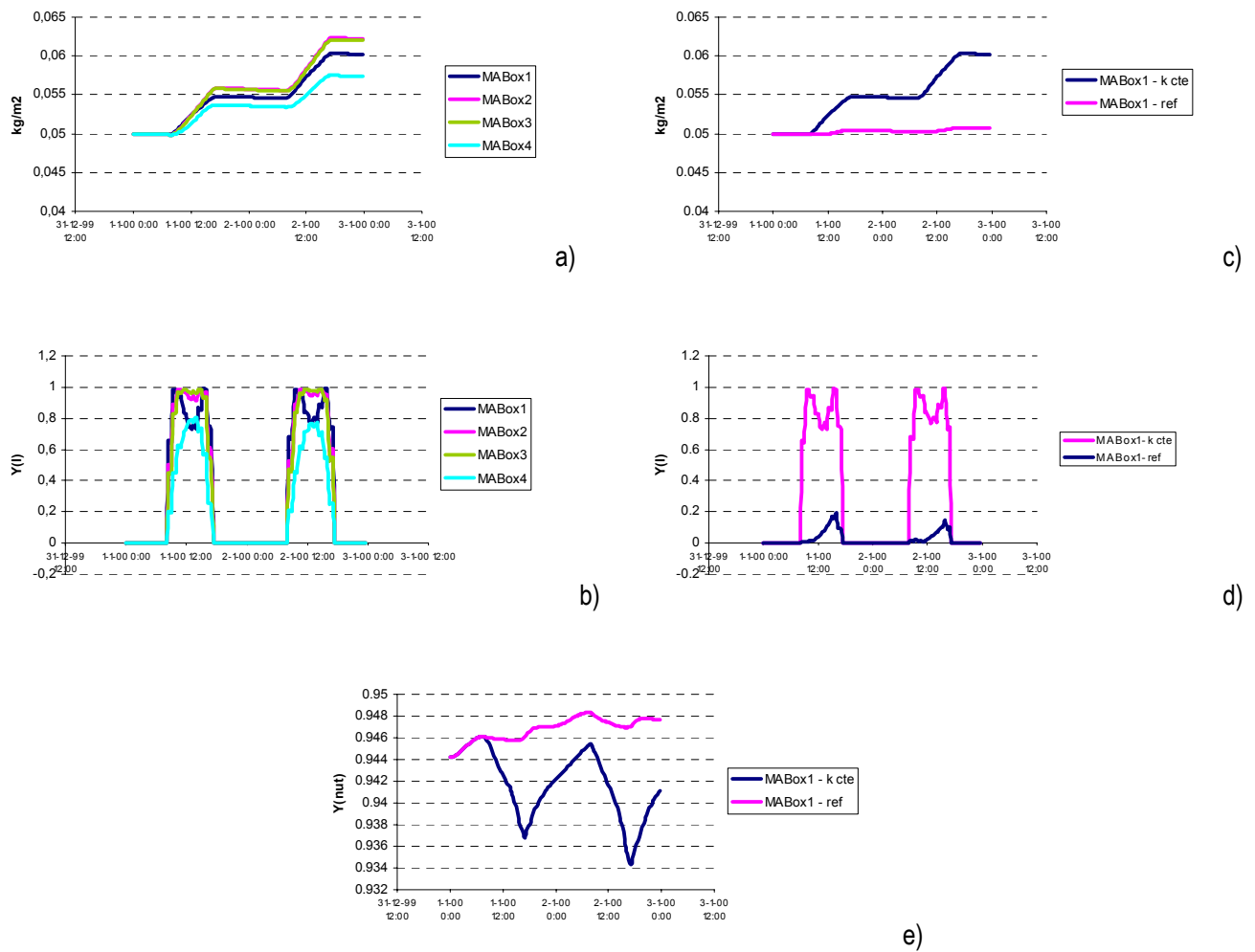


Figure 5.5 – Simulation with constant water column extinction coefficient ($k_{WC} = 0.08 \text{ m}^{-1}$): a) macroalgae biomass; b) macroalgae biomass in run A and reference run, in box 1; c) macroalgae light limitation factor; d) macroalgae light limitation factor in run A and reference run, in box 1; e) macroalgae nutrient limitation factor in run A and reference run, in box 1

In the simulation with ocean's light extinction coefficient (run B), macroalgal biomass was even higher than in the previous run but in the same order of magnitude (20.4% in the previous run and 20.7% in this one) due to the absence of photoinhibition (Figure 5.6a), in contrast to what happens for phytoplankton (Figure 5.6b). Although lower than the previous run, phytoplankton is photoinhibited at mid-day irradiances. From this run, we cannot extrapolate that overall annual growth will be higher, because this is a two-day simulation and the seasonality effect is disregarded.

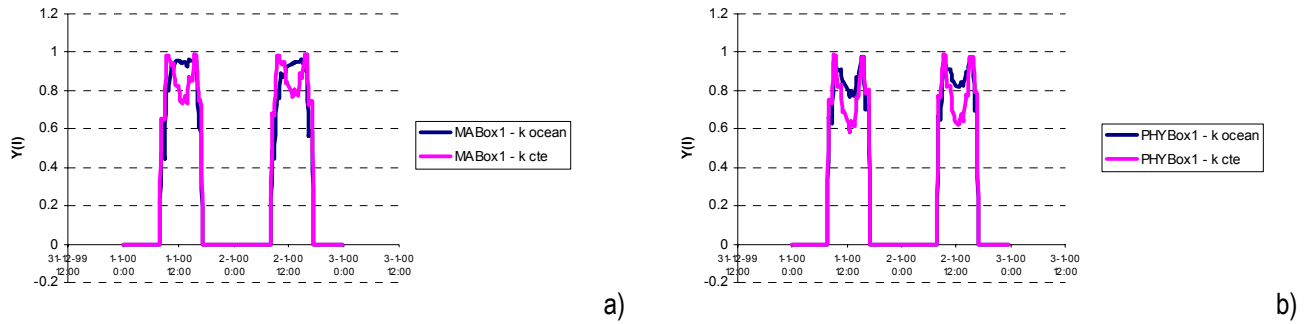


Figure 5.6 – comparison between light limitation factors in run B and the reference run, for macroalgae (a) and for phytoplankton (b)

Light limitation given by the Mediterranean coefficient (run C) does not distance so much to the reference run as the previous analysed runs. Net macroalgae's growth in box 1 is negative (- 0.15% versus 1.35 % in the reference run) as showed in Figure 5.7a. The highest slope of the curve in Figure 5.4 will decrease algal light limitation factors by half, reducing also the photoperiod.

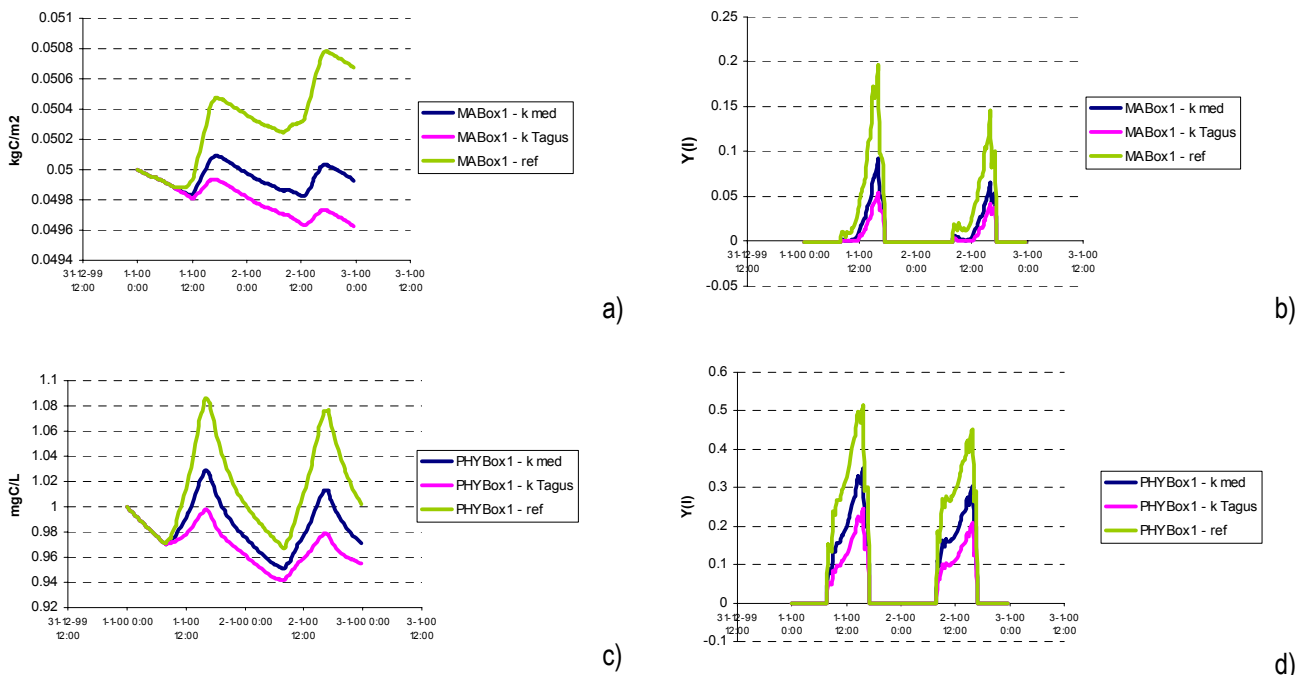


Figure 5.7 - Runs with Mediterranean and Tagus estuary light extinction coefficient; comparison with reference run: a) macroalgae biomass in box 1; b) macroalgae light limitation factor in box 1; c) phytoplankton biomass; d) phytoplankton light limitation factor in box 1.

The fourth simulation (run C) used a light extinction coefficient calibrated for Tagus Estuary (Pina, 2001 and Portela, 1996). From the plots above one can see that the inclusion of the absorption by particulate suspended material severely decreases light availability.

5.2.1 Conclusion

The analysed runs show that the water column light extinction has a non-linear effect on macroalgal growth. In runs A and B, the light extinction was decreased by approximately 90%, for an average value of 1 mgL^{-1} of phytoplankton with 60% chlorophyll content (Valiela, 1995; Pina, 2001), and led to increases in macroalgal biomass of near 20 times more than in the reference run, while the average decrease of k_{WC} in runs C and D was in the order of 66% and 175%, respectively, and led to much smaller variations in macroalgal biomass. The differences between run C and D indicate that the Mediterranean light extinction coefficient seems very limitative, even for phytoplankton.

Reducing macroalgal shading area (a_{abs}) to $1 \text{ m}^2\text{kgC}^{-1}$, with the reference light extinction in the water column, will lead to the same results as with $a_{abs} = 5 \text{ m}^2\text{kgC}^{-1}$ and doubling it gives light limitation as in run C, leading to the conclusion that incident light on the weed bed is low enough to completely control the light limitation factor. This means that low incident radiation in the weed bed will be more important in light limitation than the benthic light extinction coefficient itself.

In computing the water column light extinction coefficient, the shading effect caused by dislodged floating macroalgae can be included in the total chlorophyll amount or in the particulate matter concentration. Special careful should be taken in this choice because the experimental specific light extinction coefficients may not account for the existence of macroalgae floating fronds, being preferable to add another partial extinction coefficient in expression (3.4).

5.3 EFFECT ON DISSOLVED OXYGEN

Reference run and Run D (the most limitative) were compared with similar ones, but without macroalgae simulation to see macroalgae's influence in dissolved oxygen concentrations (Figure 5.8).

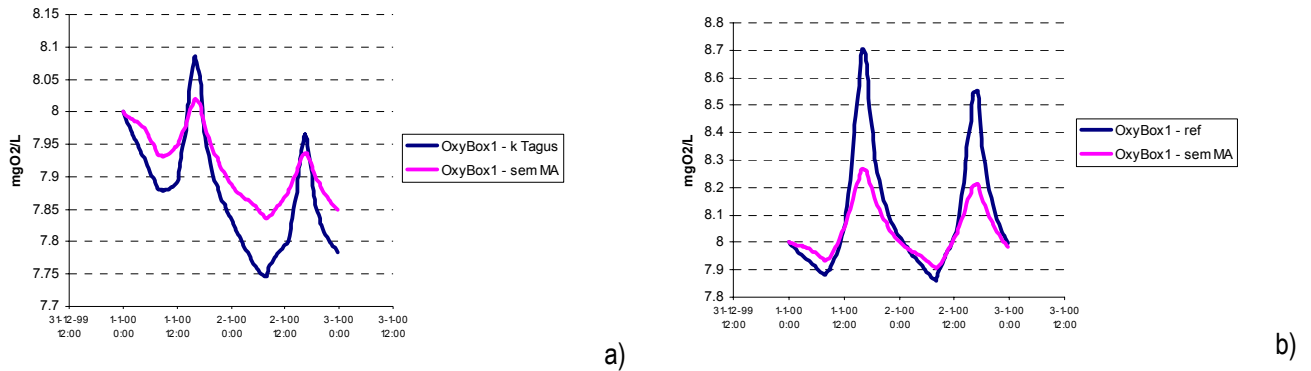


Figure 5.8 – Oxygen evolution with and without macroalgal simulation: a) in box 1 of run D; b) in box 1 of reference run

It can be verified that the presence of macroalgae increases the diurnal oxygen gradients. When macroalgae are severely limited (Figure 5.8a) the major oxygen differences occur in the night because dying macroalgae increase total organic matter oxidation, and thus, oxygen consumption. Daily oxygen production does not compensate the high night consumption, revealing that macroalgae bed will disappear in a number of days. In the reference run (Figure 5.8b), that compensation is achieved and the net balance of dissolved oxygen is positive. The macroalgae's major effect on dissolved oxygen should be analyzed with basis on diurnal oxygen variations rather than total net balance. When subject to severe light limitation, macroalgae beds tend to anoxidize the environment by the high amounts of organic matter entering the detrital food web.

5.4 MACROALGAE'S ESTABLISHMENT

A six-month simulation was made with the same conditions as in the reference run but with the benthic establishment parameters activated, with a critical detachment shear stress of 0.14 Pa and a maximum sediment deposition flux of $5 \times 10^{-3} \text{ gm}^{-3}\text{s}^{-1}$. The sediment erosion and deposition values used were 0.1 and 0.05 Pa, respectively.

The macroalgae's distribution pattern in the end of the run can be seen in **Figure 5.9**. In this run, the macroalgae's establishment criteria did not influence biomass distribution significantly because the highest shear stress areas of this estuary are at depth where macroalgae is completely light limited and the deposition fluxes are not high in the intertidal areas (**Figure 5.10** and **Figure 5.11**). In depth higher than approximately 4 m, macroalgae are light limited due to the lower values of incident light, i.e., they are limited by the water column extinction coefficient. This is in contrast with what happens in the upper intertidal areas, where macroalgae are most of the time emerged, and are light limited due to the weed bed light extinction. These results confirm the observations made by Ferreira (1989) in which macroalgae's meadows in estuaries are between 0.8 and 1.2 m above the hydrographic zero.

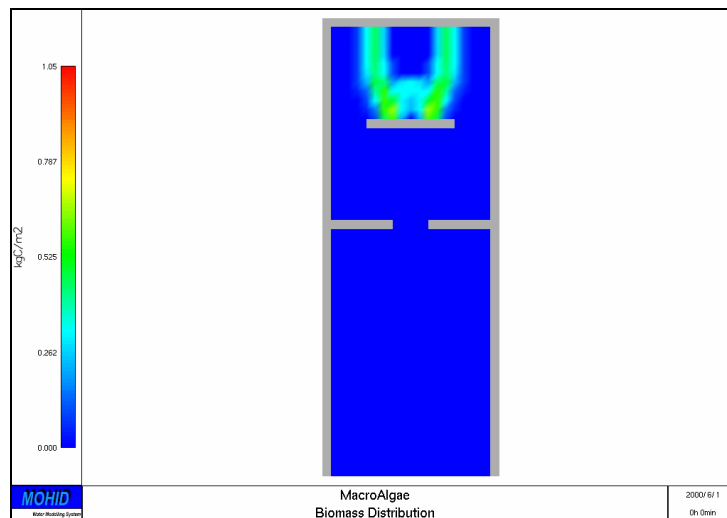


Figure 5.9 - Macroalgae distribution pattern in the schematic estuary at 2000/06/01 at 00:00.

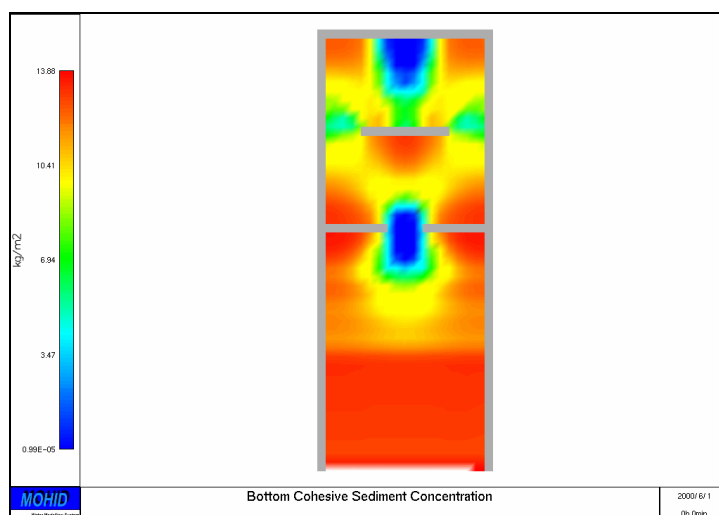


Figure 5.10 – Cohesive sediment distribution pattern in the schematic estuary at 2000/06/01 at 00:00.

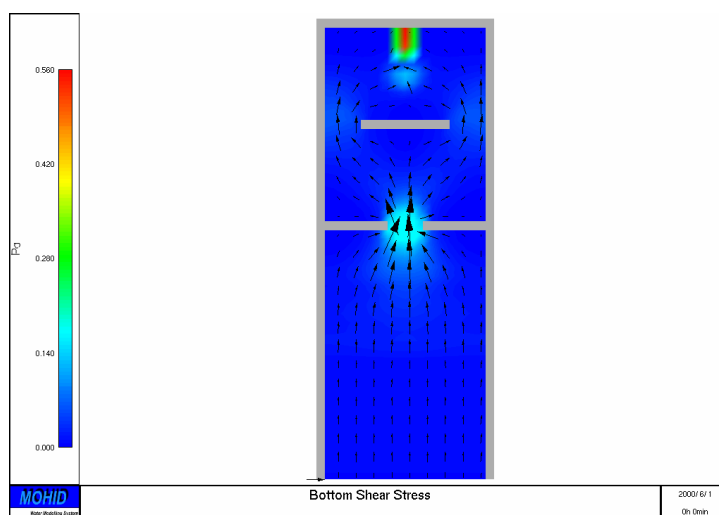


Figure 5.11 – Shear stress (color) and horizontal velocities (vectors) in the schematic estuary at 2000/06/01, 00:00.

Figure 5.12 represents the intertidal substrata zonation existing in Tagus Estuary. Macroalgae's preferential substrata are the oyster beds, leaving the upper intertidal area for vascular plants colonization. The developed model was applied to this Estuary in a five-day simulation. The initial condition used for macroalgae (5 gC.m^{-2}) was provided by experimental results in Ferreira (1989). The results are satisfactory, although mainly qualitative, and macroalgae's more intensive colonization areas (red coloured zones) are established precisely at the oyster beds. Net primary production rates were approximately $0.03 \text{ gC.m}^{-2}.\text{h}^{-1}$ for the intertidal areas being well correlated with the values given by Ferreira (mean of $0.06 \text{ gC.m}^{-2}.\text{h}^{-1}$). Deviations can be justified by the absence of other benthic primary producers in the model and by the large cell grid used ($500 \times 500 \text{ m}$). High grid size may give low productivities because the experimentally primary productivities values are usually measured within a few square meters.

One must emphasize that maximum time step is limited by the quality of the initial conditions. The model is started using an approximated initial distribution of sediments and macroalgae. These distributions are modified by sources and sinks in case of algae and by erosion/deposition followed by advection in case of sediments. In case of macroalgae, an overestimation of the initial concentration will generate over consumption of nutrients during drying processes in intertidal areas, which could generate negative concentrations of nutrients in the water column. Unrealistic concentrations can also be generated by advection also during drying periods due to the conservative properties of the model. The magnitude of both destabilization mechanisms can be minimized acting on the time step used by the model. For this reason, a smaller time step is used for model “warming up”, while inaccuracy of initial conditions is dissipated. Concomitantly a test to negative concentrations is performed in all iterations. When negative values are found, they are updated to zero and the mass generated numerically is added to an integration matrix. At the end of each run, the matrix of generated mass is evaluated. Points displaying persistent problems usually indicate the presence of unrealistic topographic discretization, generating unrealistic episodic high velocity events with associated rapid volume variations in drying intertidal areas. This will originate instabilities because the model uses a conservative approach (courant and diffusion numbers also depend on volume temporal variations). In practical terms, these problems arise in just a few points and have no consequences on the overall result. Simulations with smaller time steps and the imposition of a minimum concentration in these local problems (and the analysis of the artificially created mass afterwards) suffice to avoid this problem.

Because inter-annual and seasonal variations are needed to study water quality regimes, the usage of minor steps can lead to high computation times. Simulations with increasing time steps are a good and practical solution to this problem.

From the above discussion, it can be said that the results obtained reveal the robustness of the model by dynamically predicting macroalgae’s establishment areas in short-term simulations.

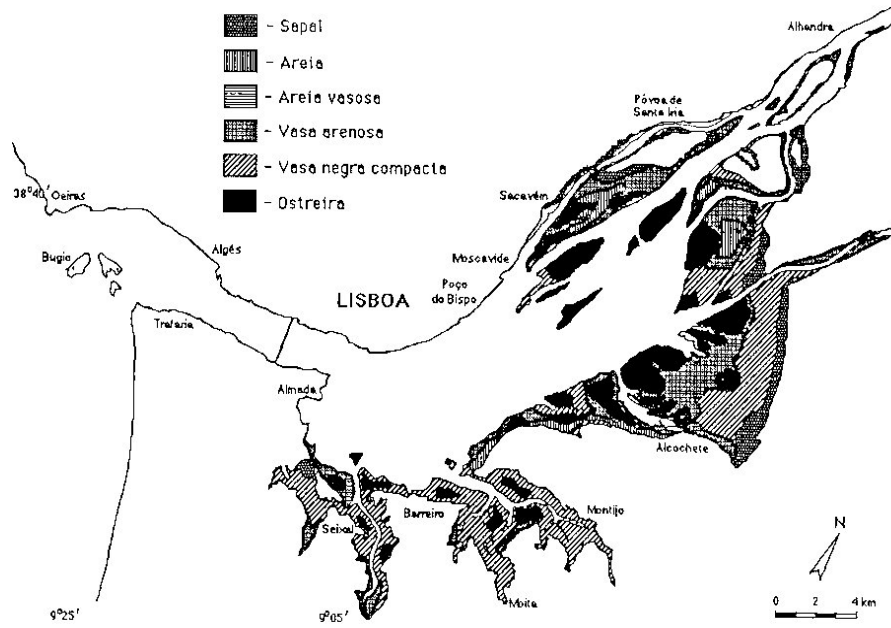


Figure 5.12 - Intertidal substrata in Tagus Estuary (After Ferreira, 1989)

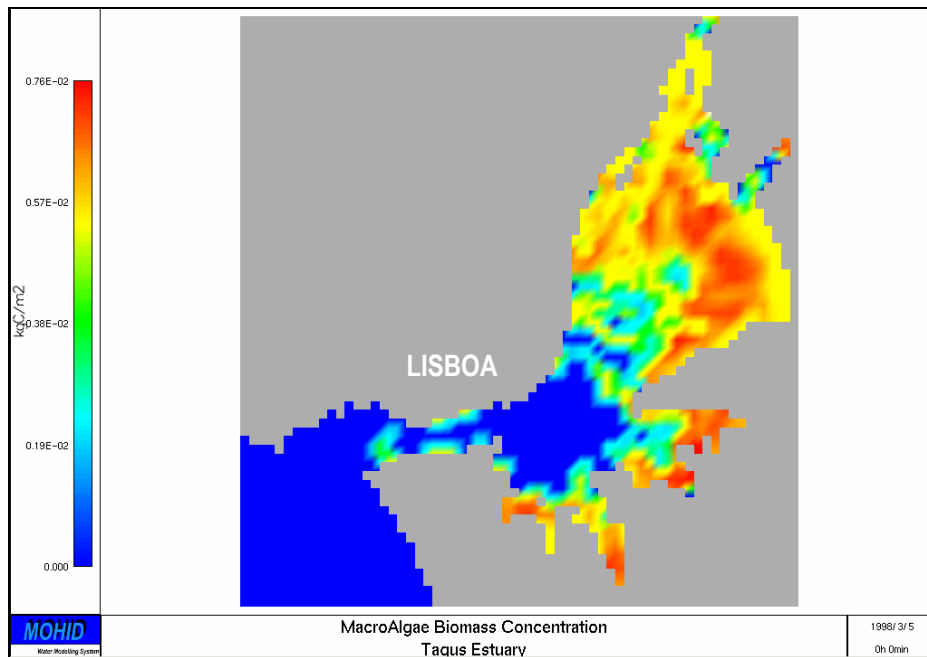


Figure 5.13 - Macroalgae distribution pattern (fifth day run)

6 CONCLUSIONS

A delicate balance between nutrient load, water velocities and light availability influences macroalgae growth. All the three are interconnected and little changes in one of them can lead to algal blooms or total destruction of seaweed bed. The developed model, being coupled with a hydrodynamic and water quality model is a useful tool in the prediction and prevention of these phenomena.

In most estuarine systems, light has a preponderant role in macroalgae production rates. The results obtained suggest that macroalgae's productivity is highly sensitive to light extinction coefficients. Several light extinction formulations were tested with the conclusion that water column formulations must be preferentially based on local experimental relationships, which should include chlorophyll and particulate matter concentration effects on water column light penetration. Macroalgae's light limitation is controlled by the water column light extinction coefficient, which determines the amount of incident radiation in the weed bed. Nevertheless, the extinction occurring in the benthic bed is a determinant factor when they are dense or partially emerged.

The developed model is designed for application in different topographic and climatographic systems because it simulates macroalgal production rates with relative accuracy and dynamically predicts macroalgae's establishment areas.

The simple approach used in the definition of macroalgae establishment areas allows an easy calibration of the model, and the possibility of simulating a wide range of macroalgal morphologic behavioural patterns.

Macroalgae are influenced by the global estuarine mechanism and their contribution to the nutrient cycling may seem a mild one because they are localized producers, with high carbon doubling times. However, macroalgae beds represent a large organic mater reservoir that increase diurnal oxygen gradients and can deeply affect the biogeochemical cycles of nutrients and oxygen when subject to extreme environmental conditions. The model developed and coupled with MOHID is able to reflect this conjugated phenomena will accuracy.

7 FUTURE RESEARCH

The validation of the implemented model by its application to several and distinct estuarine ecosystems, in long term simulation is yet to be done. Besides validating, these applications can aid in the definition of strategies for water quality management practices.

To quantify the amount of organic macroalgae exported to the ocean, a lagrangian transport model can be used to simulate advection transport of broken or dislodged algae fronds. The eulerian approach given in this work simplifies this by considering floating macroalgae as particulate non-living material, although of a more refractory nature.

Future developments of the macralgae production model can be made in the establishment criteria area by a dynamical computation of the critical detachment shear stress as a function of substrate adhesion strength, and thus, sediment deposition. This relationship may depend on the benthic boundary layer influence in bottom flow conditions and sediment dynamics. The simulation of these processes could lead to a better understanding of their role in estuarine dynamics.

The study of salinity's influence in the weed bed production and establishment processes can be interesting when river discharges and precipitation phenomenon are to be related with macroalgae development.

Many studies have been made for algal light availability parameterizations, but most of all for phytoplankton. Light availability in the benthic weed bed and its influence on macroalgae's growth is still an open and interesting area of research that currently needs some more in-depth approach.

Macroalgae production model could also be improved by the inclusion of luxury uptake, considering a variable internal C:N:P ratio. This typical macroalgae adaptation can be important in seasonal gradients simulation, because nutrient storage allows them to grow in late winter periods, when water is nutrient still depleted and photoperiod increases.

For the purpose of water quality management, toxicology effects can be easily added to this model. The implementation of a mathematical algorithm to simulate frond growth coupled with MOHID model is an interesting approach to study harvesting effects.

Nevertheless, the model developed is in the “state-of-the-art” of macroalgae production models and will be the basis for a two-year project on Mondego Estuary, in cooperation with Universidade de Coimbra, financed by Instituto da Água (INAG) from Ministério das Cidades, Ordenamento do Território e Ambiente.

8 REFERENCES

- Airoldi, L. & Cinell, F. (1997); *Effects of Sedimentation on Subtidal Macroalgal Assemblages: an Experimental Study from a Mediterranean Rocky Shore*; J. Exp. Mar. Biol. Ecol., vol. 215: 269-288
- Arhonditsis, G.; Tsirtsis, G.; Angelidis, M.; Karydis, M. (2000); *Quantification of the effects of non point nutrient sources to coastal marine eutrophication: applications to a semi-enclosed gulf in the Mediterranean Sea*; Ecol. Mod., vol.129 (2-3): 209 - 227
- Atkinson, M. & Smith, S.V. (1983); *C:N:P Ratios of Benthic Marine Plants*; Limnol. and Oceano., 28:568-574.
- Baird, M (2001); *Technical Description of the CSIRO SERM Ecological Model*; CSIRO Land and Water, Australia (www.marine.csiro.au/serm)
- Barnes, R. & Hughes, R. (1988); *An Introduction to Marine Ecology*; Blackwell Science, 2nd Edition.
- Bell (1993) "Photosynthetic response to temperature and dessication of the intertidal alga *Mastocarpus papillatus*", Marine Biology 177: 337-346
- Carr, G; Duthie, H.; Taylor, W. (1997); *Models of Aquatic Plant Productivity: A Review of the Factor that Influence Growth*; Aquatic Botany, vol. 59: 195-215.
- Cheshire, A.; Miller, D.; Stewart, R. (1999); *Effect of dispersed sediment plumes from beach sand replenishment dredging on recruitment of phaeophycean algae to rocky reefs in Gulf St. Vincent, South Australia*; Department of Environmental Biology, University of Adelaide, Australia
- Christian, G. (1986); *Analytical Chemistry*; John Wiley & Sons, 4th Edition
- Coffaro, G. & Sfriso, A. (1997); *Simulation Model of Ulva rigida in shallow water of the Lagoon of Venice*; Ecological Modelling, vol. 102: 55-66.
- Coffaro, G. & Bocci, M. (1997); *Resources Competition between Ulva rigida and Zoostera marina: a quantitative approach applied to the Lagoon of Venice*; Ecological Modelling, vol. 102: 81-95.
- Dronkers, J. & Leussen, W. (1988); *Physical Processes in Estuaries*; Springer-Verlag

Enriquez, S.; Agustí, S. Duarte, C. (1994); *Light Absorption by Marine Macrophytes*; *Oecologia*, vol. 98: 121-129.

EPA (1985) Rates, Constants and Kinetics Formulations in Surface Water Quality Modelling (2nd Edition); United States Environmental Protection Agency, Report EPA/600/3-85/040.

Falkowsky, P.G. (2000); *Racionalizing elemental ratios in unicellular algae*; *J. Phycol.*, 36:3-6

Fernandes, L. (2001); *Transporte de Poluentes em Estuários* Trabalho Final de Curso da Licenciatura em Engenharia do Ambiente, Instituto Superior Técnico, Universidade Técnica de Lisboa.

Ferreira, J. (1989); *Mercúrio em algas macrófitas do Estuário do Tejo*; Dissertação apresentada à Universidade Nova de Lisboa para obtenção do grau de Doutor em Ciências do Ambiente, Lisboa.

Finlay, J.; Callow, M.; Schultz, M.; Swain, G.; Callow, J. (2002); *Adhesion Strength of Settled Spores of the Green Alga Enteromorpha*; *Biofouling*, vol. 18 (4): 251-256

Fonseca M. & Kenworthy, W. (1987); *Effects of Current on Photosynthesis and Distribution of Seagrasses*; *Aquatic Botany*, 27; 59 – 78.

Gotelli, N. (1995); *A Primer of Ecology*, Sinauer Associates, Inc., USA.

Hamilton & Herzfeld, *Computational Aquatic Ecosystem Dynamics Model: A Science Manual*, Centre for Water Research, The University of Western Australia Nedlands, Australia (http://www.cwr.uwa.edu.au/services/models/CAEDYM/documentation/scienceGuide/caedym_science.html)

Hurd, C. (2000); *Water Motion, Marine Macroalgal Physiology, and Production*; *J. Phycol.* vol. 36: 453 – 472

Jones, A. (1993); *Macroalgal Nutrient Relationships*; A literature review submitted to the Department of Botany, University of Queensland, in partial fulfilment of the requirements of the Honours Degree of the Bachelor of Science.

Kaandorp, J. & Kübler, J. (2001); *The Algorithmic Beauty of Seaweeds, Sponges and Corals*; The Virtual Laboratory; Springer-Verlag

Kröncke, I.; Bergfeld, C. (2001); *Synthesis and New Conception of North Sea Research, Working Group 10: Review of the Current Knowledge on North Sea Benthos*, Hamburg University

Krone, R. (1962); *Flume Studies of the Transport in Estuaries Shoaling Processes*; Hydr. Eng. Lab.; University of Berkeley, California, USA.

Little C. & Kitching J.A. (1996); *The Biology of Rocky Shores*; Biology of Habitats, Oxford University Press

Mann, K. (1982); *Ecology of Coastal Waters – A Systems Approach*; Studies in Ecology, vol. 8; Blackwell Scientific Publications

Marques, J.; Rodrigues, L.; Nogueira, A. (1993); *Intertidal Macrobenthic Communities Structure in the Mondego Estuary (Western Portugal): Reference Situation*; Vie Millieu, vol. 43 (2-3): 177-187

Martins, I; Pardal, M.; Lillebo, A.; Flindt, M.; Marque, J. (2001); *Hydrodynamics as a Major Factor Controlling the Occurrence of Green Macroalgal Blooms in a Eutrophic Estuary: A Case Study on the Influence of Precipitation and River Management*; Estuarine, Coastal and Shelf Science, vol. 52: 165-177

Miranda, R.; Braunschweig, F; Leitão, P.; Neves, R.; Martins, F.; Santos, A.(2000); *MOHID2000 – A Coastal Integrated Object Oriented Model*; in Blain, W. & Brebbia, C.; *Hydraulic Engineering Software VII*; WIT Press.

MOHID (2000); *MOHID Description*; MARETEC, Instituto Superior Técnico, Universidade Técnica de Lisboa.

Moon, D. (2001/2002); *Lectures on Marine Botany*, UCSC Biological Sciences Course Materials , Biology course 170 & 170L, University of California, Department of Biology, Santa Cruz, California (<http://bio.classes.ucsc.edu/bio170/lecture3.html>)

Parsons, T.; Takahashi M.; Hargrave B; (1984) *Biological Oceanographic Processes*; Butterworth-Heinemann Ltd.

Partheniades, E. (1965); *Erosion and Deposition of Cohesive Soils*; J. HYdr. Div.; ASCE, 91, N°. HY1: 105-139

Phillips, T. (1999); *Harmonic Analysis and Prediction of Tides*

(<http://www.math.sunysb.edu/~tony/tides/harmonic.html>)

Pina, P. (2001); *An Integrated Approach to Study the Tagus Estuary Water Quality*; Dissertação para obtenção do grau de Mestre em Ecologia, Gestão e Modelação dos Recursos Marinhos; Instituto Superior Técnico, Universidade Técnica de Lisboa.

Portela, L. (1996); *Modelação Matemática de Processos Hidrodinâmicos e de Qualidade da Água no Estuário do Tejo*; Dissertação para obtenção do grau de Doutor em Engenharia do Ambiente; Instituto Superior Técnico, Universidade Técnica de Lisboa.

Ré, P. (1996/1997); *Biologia Marinha*; Associação dos Estudantes da Faculdade de Ciências de Lisboa, Universidade de Lisboa.

Rivera, P. (1997); *Hydrodynamics, Sediment Transport and Light Extinction of Cape Bolinao, Philippine*; PhD Dissertation; A.A. Balkema/Rotterdam/Brookfield

Salomonsen, J.; Flindt, M.; Geertz-Hansen, O.; Johansen, C. (1999); *Modelling Advective Transport of Ulva lactuca (L) in sheltered bay, Møllekrogen, Roskilde Fjord, Denmark*; Hydrobiologia, vol. 00: 1-13

Steele, J. (1962); *Environmental Control of Photosynthesis in the Sea*; Limnology and Oceanography, vol.7: 137-150.

Thornton, K. & Lessen, A. (1978); *A Temperature Algorithm for Modifying Biological Rates*; Trns. Am. Fish. Soc., vol. 107 (2): 284-287

Valiela, I. (1995); *Marine Ecological Processes*; Springer-Verlag, New York, 2nd Edition.

APPENDIX

APPENDIX INDEX

I NOMENCLATURE ON MARINE SYSTEMS	I.1
I.1 DIVISION CATEGORIES	I.1
I.2 BENTHIC SYSTEM	I.1
I.3 ALGAL TYPES	I.2
II DATA HANDLING	II.1
II.1 GRAPHICAL USER INTERFACE	II.1
II.2 VISUAL BASIC MACROS	II.2
III HYDRODYNAMIC TRANSPORT IN MOHID	III.1
IV CONSERVATION LAW OF A SCALAR PROPERTY	IV.1
V ECOLOGICAL MODEL EQUATIONS	V.1
V.1 STATE VARIABLES:	V.1
V.2 AUTOTROPHS	V.2
V.2.1 <i>Phytoplankton</i>	V.2
V.2.1.1 Light Limiting Factor	V.3
V.2.2 <i>MacroAlgae</i>	V.4
V.2.2.1 Light Limiting Factor	V.5
V.2.3 <i>Nutrients Limitation Factor</i>	V.5
V.2.4 <i>Respiration</i>	V.5
V.2.5 <i>Excretion</i>	V.6
V.2.6 <i>Natural Mortality</i>	V.6
V.3 ZOOPLANKTON	V.7
V.4 NITROGEN CYCLE	V.8
V.4.1 <i>Ammonia</i>	V.8
V.4.2 <i>Nitrite</i>	V.10
V.4.3 <i>Nitrate</i>	V.10
V.4.4 <i>Particulate Organic Nitrogen</i>	V.11
V.4.5 <i>Non-Refractory Dissolved Organic Nitrogen</i>	V.12
V.4.6 <i>Refractory Dissolved Organic Nitrogen</i>	V.13
V.5 PHOSPHOROUS CYCLE	V.14
V.5.1 <i>Inorganic Phosphorus</i>	V.14
V.5.2 <i>Particulate Organic Phosphorus</i>	V.15
V.5.3 <i>Non-Refractory Dissolved Organic Phosphorus</i>	V.16
V.5.4 <i>Refractory Dissolved Organic Phosphorus</i>	V.17
V.6 OXYGEN CYCLE	V.18
V.7 TEMPERATURE EFFECT	V.19
V.8 EXCRETION FRACTIONS	V.20
VI PARAMETERS LIST	VI.1

APPENDIX I

I NOMENCLATURE ON MARINE SYSTEMS

I.1 DIVISION CATEGORIES

Regardless of their phylogenetic position, marine organisms can be placed in two large categories dependent on whether they live in the water mass (pelagic) or on or in the bottom sediments or rock (benthic). A minor, third category is required for those organisms that straddle the air-water interface (pleustic). Pelagic organisms can yet be divided into two categories: nektonic with swimming organisms, and planktonic with drifting organisms. All these categories, although extremely useful, are by no means mutually exclusive or rigidly definable. Some species are benthic as adult but pelagic as larvae, and a number of pelagic organisms may spend much time resting on or feeding at the sediment-water interface (these are often termed benthopelagic). (Barnes & Hughes, 1988).

Each category forms a system characterized by specific ecological functions. The **pelagic system** comprises the water column, the pelagic organisms and the processes that occur within, while the **benthic system** comprises the benthic communities, the sediments and water-sediment interface, and the processes that occur within.

I.2 BENTHIC SYSTEM

In marine environments, the benthic system is usually divided in several regions or levels¹. All the zonation systems proposed are based on the composition and modifications of the benthic communities and not on physical-chemical factors. According to Pèrès (1961, in Ré, 1996/1997) the several levels of the benthic system can be grouped in two main systems: the *littoral system* and the *deep system*. The first comprises the levels in which autotrophic vegetation grows and the second comprises the bathial, abyssal and hadal levels.

The littoral system can be divided in (1) the *upper tidal* characterized by benthic communities that demand or support a continuous state of emersion, being immersed only exceptionally; (2) the *intertidal* level is characterized by communities that support or need periodic emersion and immersion states; (3) and the

¹ A level is a vertical region of the domain where ecological conditions, which depend on the relative position to the mean surface water level, are constant or vary between two levels that mark their limits.

subtidal level colonized by communities that support or need continuous immersion states, being emersed only exceptionally. The lower limit of the littoral level is given by the compatible depth with the live of photofile or zoosterian algae (15-20m in high latitudes, 30/40 m in the Mediterranean and 24 m on the Portuguese coast).

I.3 ALGAL TYPES

There are several growth algal types and each one can be identified by a specific name, being usually more useful than the taxonomic categorization. The most commonly used are listed in **Table A I.1** and are presented in this work to avoid the confusion they may cause by their similitude.

Algal Type	Definition
Phytoplankton	Microscopic Algae suspended in the open water column or pelagic zone
Metaphyton	Floating macroscopic algae
Periphyton	Algae that grow attached to substrata
Epiphytic	Periphytic algae that grow attached to other plants
Epipsammic	Periphytic algae that grow on sand
Epipellic	Periphytic algae that grow on mud (sediment)
Endopelic	Periphytic algae that grow within mud (sediment)
Epilithic	Periphytic algae that grow on rock surfaces
Endolithic	Periphytic algae that grow within cavities of rock.
Epizoic	Periphytic algae that grow attached to animals
Fouling	Periphytic algae that grow attached to objects placed in the sea

Table A I.1– Categorization and definition of algal growth types

APPENDIX II

II DATA HANDLING

II.1 GRAPHICAL USER INTERFACE

MOHID users have the possibility of analysing and visualizing input parameters and the large amount of data produced in a graphical interface developed by MARETEC's personnel. Input parameters are given by specific keywords created in ASCII files and the options can be easily defined in proper dialog boxes through this graphical interface (Figure II.1)

Simulation results can be visualized in (1) time series for a given property in specified individual cells or integrated in a box set of cells, and (2) in the matricial form for the all computational domain. The first type of data is produced in ASCII files, easily transported to spreadsheets application like MSEXcel, allowing the user to create time series plots of property concentration in the specified cells or property fluxes between sets of cells. The second type of results is produced in HDF files (*Hierarchical Data Format*) and can be visualized through vector or colour isolines or contour plots of any simulated property allowing the spatial characterization and sequential animation of these results.

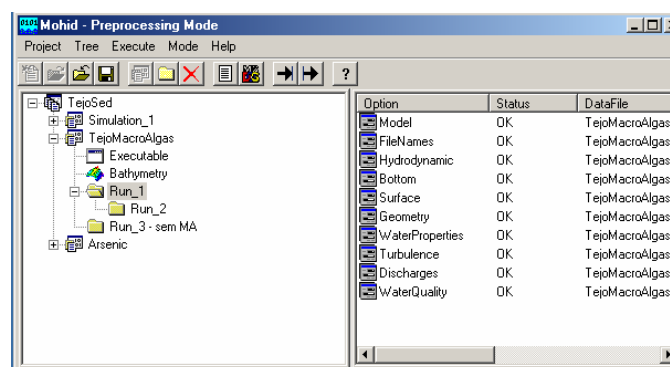


Figure II.1 – MOHID Graphical User Interface

II.2 VISUAL BASIC MACROS

The data produced can be spread in several ASCII files created by a simulation run that must be organized by the user, according to his purposes. This revealed to be a time and resource consumer task especially in the initial phase of test runs. The development of expeditious data treatment methodologies was imperative and some macros were developed in Visual Basic for Applications (VBA) programming language. The macros developed allow the comparison of user specified type of data produced by several simulations in the same MExcel book and in the same graphic plot, with the possibility of keeping original values, reducing error probability and increasing the macro's flexibility to other uses. As mentioned in **Chapter 4** the macros developed are available to all other users of MOHID. Although macros are specifically directioned programs, adjustments can be easily made by the user. Some of the user forms created can be visualized in **Figure II.2**.

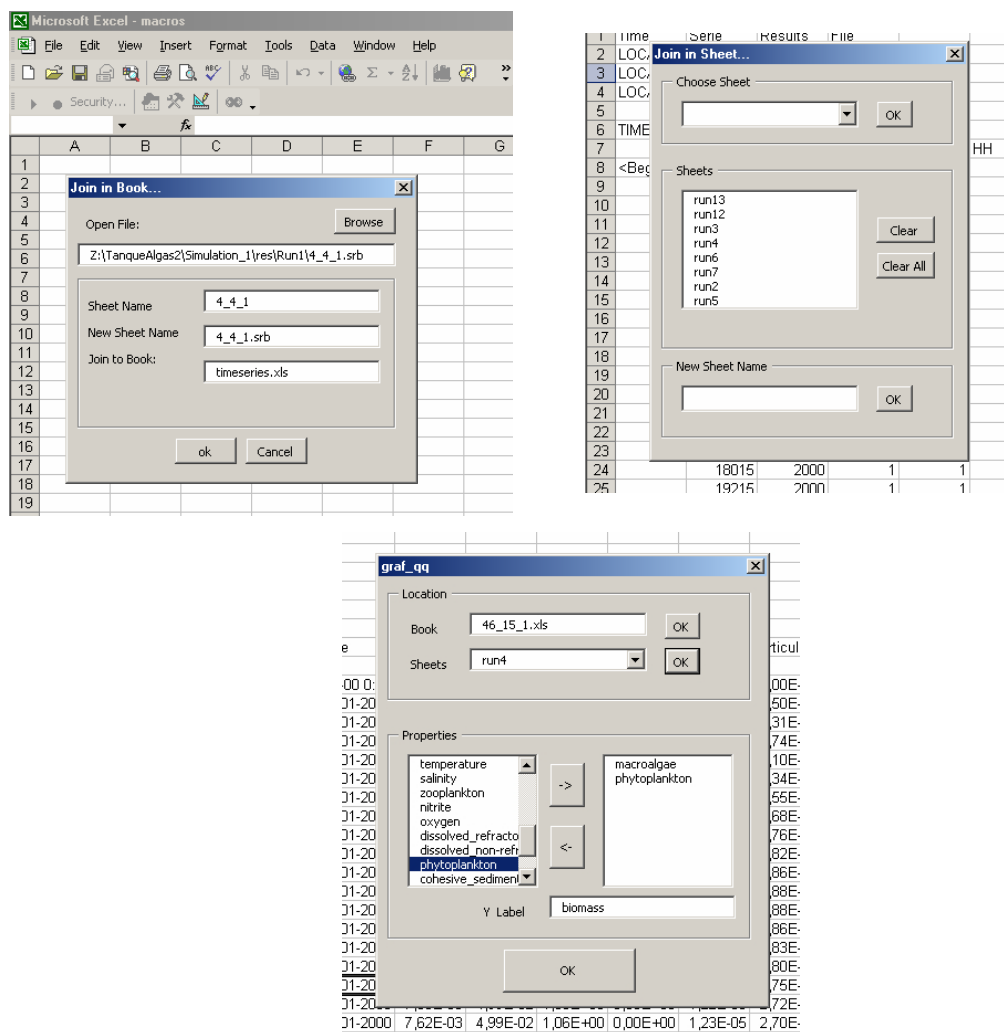


Figure II.2 – UserForms of the macros developed

APPENDIX III

III HYDRODYNAMIC TRANSPORT IN MOHID

MOHID model solves the three-dimensional incompressible primitive equations of momentum transport, assuming hydrostatic equilibrium as well as Boussinesq and Reynolds approximations. All the equations below have been derived taken into account these approximations. The momentum balance equations for mean flow horizontal velocities are, in cartesian form:

$$\begin{aligned} \frac{\partial u}{\partial t} = & -\frac{\partial(uu)}{\partial x} - \frac{\partial(uv)}{\partial y} - \frac{\partial(uw)}{\partial z} + fv - \frac{1}{\rho_0} \frac{\partial p}{\partial x} + \\ & + \frac{\partial}{\partial x} \left((v_H + \nu) \frac{\partial u}{\partial x} \right) + \frac{\partial}{\partial y} \left((v_H + \nu) \frac{\partial u}{\partial y} \right) + \frac{\partial}{\partial z} \left((v_t + \nu) \frac{\partial u}{\partial z} \right) \end{aligned} \quad (\text{A III.1})$$

$$\begin{aligned} \frac{\partial v}{\partial t} = & -\frac{\partial(vu)}{\partial x} - \frac{\partial(vv)}{\partial y} - \frac{\partial(vw)}{\partial z} - fu - \frac{1}{\rho_0} \frac{\partial p}{\partial y} + \\ & + \frac{\partial}{\partial x} \left((v_H + \nu) \frac{\partial v}{\partial x} \right) + \frac{\partial}{\partial y} \left((v_H + \nu) \frac{\partial v}{\partial y} \right) + \frac{\partial}{\partial z} \left((v_t + \nu) \frac{\partial v}{\partial z} \right) \end{aligned} \quad (\text{A III.2})$$

Where u , v and w are the components of the velocity vector in the x , y and z directions respectively, f the Coriolis parameter, v_H and v_t the turbulent viscosities in the horizontal and vertical directions, ν is the molecular kinematic viscosity (equal to $1.3 \times 10^{-6} \text{ m}^2\text{s}^{-1}$), p is the pressure. The temporal evolution of velocities (term on the left hand side) is given by the balance of advective transports (first three terms on the right hand side), Coriolis force (forth term), pressure gradient (next three terms) and turbulent diffusion (last three terms).

The vertical velocity is calculated from the incompressible continuity equation (mass balance equation):

$$\frac{\partial u}{\partial x} + \frac{\partial v}{\partial y} + \frac{\partial w}{\partial z} = 0 \quad (\text{A III.3})$$

Integrating between bottom and the depth z , w is to be calculated:

$$w(z) = -\frac{\partial}{\partial x} \int_{-h}^z u dx - \frac{\partial}{\partial y} \int_{-h}^z v dy \quad (\text{A III.4})$$

Thus, the free surface equation is obtained by integrating the equation of continuity over the whole water column (between the free surface elevation $\eta(x,y)$ and the bottom $-h$):

$$\frac{\partial \eta}{\partial t} = -\frac{\partial}{\partial x} \int_{-h}^{\eta} u dz - \frac{\partial}{\partial y} \int_{-h}^{\eta} v dz \quad (\text{A III.5})$$

The hydrostatic approximation is assumed with:

$$\frac{\partial p}{\partial z} + g\rho = 0 \quad (\text{A III.6})$$

where g is gravity acceleration and ρ is density. If the atmospheric pressure p_{atm} is subtracted from p , and density ρ is divided into a constant reference density ρ_0 and a deviation ρ' from that constant reference density, after integrating from the free surface to the depth z where pressure is calculated, we arrive to:

$$p(z) = p_{atm} + g\rho_0(\eta - z) + g \int_z^{\eta} \rho' dz \quad (\text{A III.7})$$

Equation (A III.7) relates pressure at any depth with the atmospheric pressure at the sea surface, the sea level and the anomalous pressure integrated between that level and the surface. By using this expression and the Boussinesq approximation, the horizontal pressure gradient in the direction x_i can be divided in three contributions:

$$\frac{\partial p}{\partial x_i} = \frac{\partial p_{atm}}{\partial x_i} - g\rho_0 \frac{\partial \eta}{\partial x_i} - g \int_z^{\eta} \frac{\partial \rho'}{\partial x_i} dz \quad (\text{A III.8})$$

The total pressure gradient is the sum of the gradients of atmospheric pressure, of sea surface elevation (barotropic pressure gradient) and of the density distribution (baroclinic pressure gradient). This decomposition of the pressure gradient is substituted in equations (A III.1) and (A III.2) .

Density is can be computed as function of these temperature and salinity properties through the following expression:

$$\rho = (5890 + 38T - 0.375T^2 + 3S) / ((1779.5 + 11.25T - 0.0745T^2) - (3.8 + 0.01T)S + 0.698(5890 + 38T - 0.375T^2 + 3S)) \quad (\text{A III.9})$$

The model resolves optionally the temperature(T) and salinity (S) transport in the water properties module.

The discretization method applied is based on a finite volume approach and uses the alternating-direction-implicit (ADI) technique. The horizontal transport and the coriolis term are computed by the explicit method, while the pression and vertical transport are computed with an implicit algorithm.

In the bottom, shear stress can be computed with the assumption of a logarithmic velocity gradient:

$$\tau = C_d |\vec{u}_+| \vec{u}_+ \quad (\text{A III.10})$$

$$C_d = k^2 \left(\text{Ln} \frac{z_+}{z_0} \right) \quad (\text{A III.11})$$

Where τ is the bottom shear stress, \vec{u}_+ is the velocity field at a distance z_+ above the bottom, C_d is the roughness coefficient, k is the Von Karman constant and z_0 is the physical rugosity height.

In the free surface, momentum flux is also imposed in the form of shear stress.

APPENDIX IV

IV CONSERVATION LAW OF A SCALAR PROPERTY

Similarly to what has been described in **appendix III** for a vectorial property as momentum, the conservation for a scalar property field (Φ) acting on a given volume V fixed in space within a vectorial velocity field \vec{v} , limited by surface S , is:

$$\frac{\partial}{\partial t} \int_V \Phi dV + \underbrace{\int_S \vec{F} \cdot d\vec{S}}_{\substack{\text{convective and} \\ \text{diffusive flux}}} = \underbrace{\int_V (F - P) dV}_{\substack{\text{sinks}(P) \text{ and} \\ \text{sources}(F)}} \quad (\text{A IV.1})$$

Applying Gauss theorem,

$$\frac{\partial \Phi}{\partial t} + \nabla \cdot \vec{F} = (F - P) \quad (\text{A IV.2})$$

With:

$$\begin{aligned} \vec{F}_C &= \Phi \vec{v} \\ \vec{F}_D &= -D \vec{\nabla} \Phi \end{aligned}$$

where \vec{F}_C and \vec{F}_D are the convective and diffusive flux, respectively, and D is the diffusivity of the property in the medium. These equations result in:

$$\frac{\partial \Phi}{\partial t} + \nabla \cdot (\Phi \vec{v}) = \nabla \cdot (D \vec{\nabla} \Phi) + (F - P) \quad (\text{A IV.3})$$

For an incompressible fluid, density is a constant and the continuity equation establishes that:

$$\frac{\partial}{\partial t} \int_V \rho dV + \int_S \rho \vec{v} \cdot d\vec{S} = 0 \Leftrightarrow \frac{\partial \rho}{\partial t} + \nabla \cdot (\rho \vec{v}) = 0 \Leftrightarrow \nabla \cdot \vec{v} = 0 \quad (\text{A IV.4})$$

By transformation of the divergence operator ($\nabla \cdot (\Phi \vec{v}) = \Phi \nabla \cdot \vec{v} + \vec{v} \cdot \nabla \Phi = \vec{v} \cdot \nabla \Phi$), and substituting in equation (A IV.3):

$$\underbrace{\frac{\partial \Phi}{\partial t} + \vec{v} \cdot (\nabla \Phi)}_{\frac{D\Phi}{Dt}} = D\nabla^2 \Phi + (F - P) \quad (\text{A IV.5})$$

In MOHID, water properties like nutrients, phytoplankton and other organic matter pools concentration are scalar properties whose fields are computed in Water Properties Module. This module solves in different modules the advection-diffusion processes (Module Advection-Diffusion), the bottom fluxes (if any) (Bottom Module Bottom) and the sinks and sources terms (Module Water Quality). This last module has a zero-dimensional approach for all finite volumes in the domain and computations are made for the following equation:

$$\frac{\partial \Phi}{\partial t} = (F - P) = K_{net} \Phi \quad (\text{A IV.6})$$

Exponential laws given by homogeneous first-order differential equations are commonly applied to the description of population growth processes (Gotelli, 1995). The formulations for the net rate K_{net} at which these processes occur have many different approaches that are described in appendix V.

As a part of the benthic system, macroalgae are a two dimensional property exchanging nutrients, carbon and oxygen from the near bottom bed to the water column. Thus, equation (A IV.5) is reduced to a temporal variation on the left side and the sinks and sources term on the right side. These bottom fluxes are computed in the Bottom module.

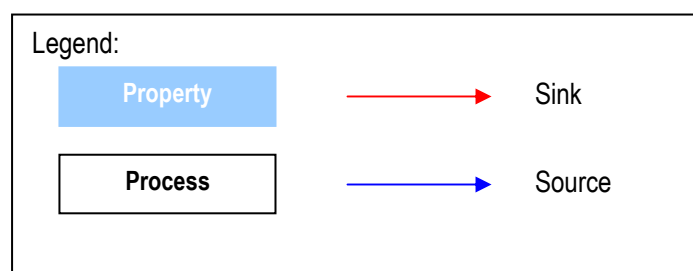
APPENDIX V

V ECOLOGICAL MODEL EQUATIONS

In this appendix, a summary of the ecological model formulations is presented, with the respective input keywords. This guide was the outcome of the need of a global understanding of the water quality model, to conveniently and consonantly develop macroalgae production model, as the basis of a future benthic model implementation.

V.1 STATE VARIABLES:

Variable	Definition	Unit
Φ_{phy}	Phytoplankton concentration	mgC.L ⁻¹
Φ_{zoo}	Zooplankton concentration	mgC.L ⁻¹
Φ_{NH4}	Ammonia concentration	mgC.L ⁻¹
Φ_{NO2}	Nitrite concentration	mgC.L ⁻¹
Φ_{NO3}	Nitrate concentration	mgN.L ⁻¹
Φ_{PON}	Particulate organic nitrogen concentration	mgN.L ⁻¹
Φ_{DONre}	Refractory dissolved nitrogen organic concentration	mgN.L ⁻¹
Φ_{DONnr}	Non-refractory dissolved nitrogen organic concentration	mgN.L ⁻¹
Φ_{IP}	Inorganic phosphorus (PO ₄ ³⁻) concentration	mgP.L ⁻¹
Φ_{POP}	Particulate organic phosphorus concentration	mgP.L ⁻¹
Φ_{DOPre}	Refractory dissolved phosphorus concentration	mgP.L ⁻¹
Φ_{DOPnr}	Non-refractory dissolved phosphorus concentration	mgP.L ⁻¹
Φ_{MA}	Macroalgae concentration	kgC.m ⁻²



V.2 AUTOTROPHS

V.2.1 Phytoplankton

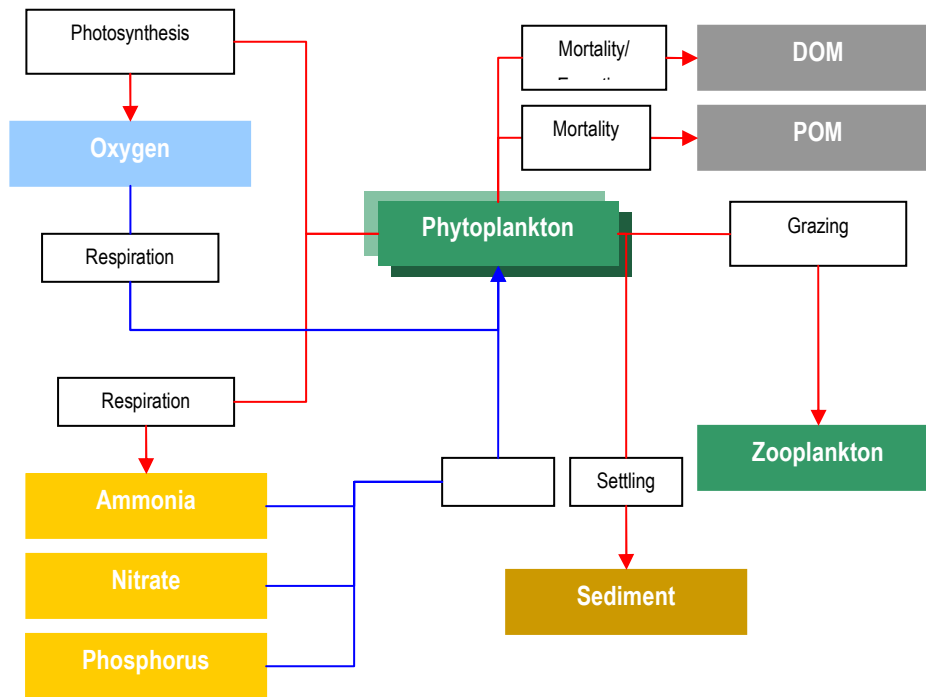


Figura V.1– Internal flux of phytoplankton

$$\frac{\partial \Phi_{phy}}{\partial t} = (\mu_{phy} - r_{phy} - ex_{phy} - m_{phy}) \Phi_{phy} - G_{zoo}^{phy} \Phi_{zoo} \quad (V.1)$$

μ_{phy} – phytoplankton gross growth rate [day⁻¹];

r_{phy} – phytoplankton total respiration rate [day⁻¹];

ex_{phy} – phytoplankton excretion rate [day⁻¹];

m_{phy} – phytoplankton natural mortality rate (non-predatory) [day⁻¹];

G_{zoo}^{phy} – zooplankton grazing rate on phytoplankton [day⁻¹];

$$\mu_{phy} = \mu_{max}^{phy}(T_{ref}) \cdot \Psi(T) \cdot \Psi(I) \cdot \text{Min}(\Psi(N), \Psi(P)) \quad (V.2)$$

$\mu_{max}^{phy}(T_{ref})$ – maximum gross growth rate at the reference temperature

GROWMAXF

$\Psi(T)$ – temperature limitation factor²

$\Psi(I)$ – light limitation factor

$\Psi(N)$ – nitrogen limitation factor

$\Psi(P)$ – phosphorus limitation factor

² See appendix V.7

$$G_{zoo}^{phy} = \frac{\mu_{zoo}}{E} \quad (V.3)$$

μ_{zoo} – zooplankton gross growth rate [day⁻¹]

E – assimilation efficiency of the phytoplankton by the zooplankton [adim]

ASS_EFIC

V.2.1.1 Light Limiting Factor

$$\Psi(I) = \frac{e}{k \cdot z} \left(e^{-I_0 e^{-kz} / I_{opt}} - e^{-I_0 / I_{opt}} \right) \quad (V.4)$$

z – vertical position (cell vertical thickness)

I_0 – incident radiation [W/m²]

I_{opt} – optimum light intensity for phytoplankton photosynthesis [W/m²]

k – light extinction coefficient in the water column.

PHOTOIN

$$k = k_w + k_c \times Chla + k_s C_{ss} \quad (V.5)$$

$$Chla = \Phi_{phy} \frac{1}{60} \times 1000 \quad (V.6)$$

k_w – water light extinction coefficient [m⁻¹]

SW_KW

k_c – chlorophyll light extinction coefficient [m⁻¹]

SW_KC

k_s – solid suspended matter light extinction coefficient [m⁻¹]

SW_KS

Chla – chlorophyll a concentration [mgChla.m⁻³]

C_{ss} – solid suspended matter concentration (sum of SPM properties concentration)

Properties that can be SPM:

- Cohesive sediment
- Particulate organic nitrogen
- Particulate organic phosphorus
- Phytoplankton
- Zooplankton

V.2.2 MacroAlgae

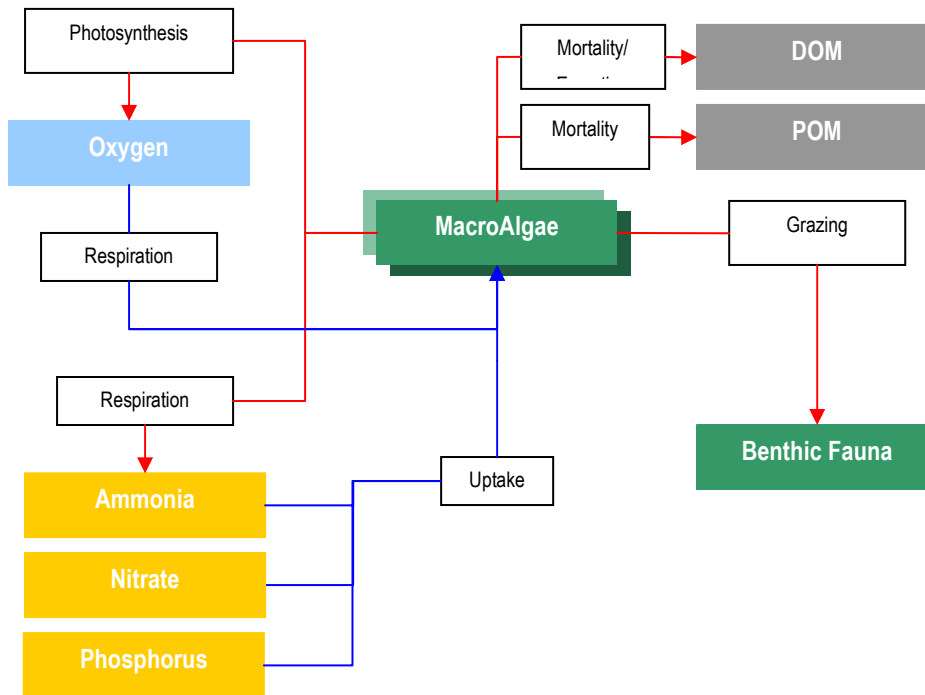


Figura V.2 – Internal flux of MacroAlgae

$$\frac{\partial \Phi_{MA}}{\partial t} = (\mu_{MA} - r_{MA} - ex_{MA} - m_{MA} - G_{MA}) \Phi_{MA} \quad (V.7)$$

μ_{MA} – macroalgae gross growth rate [day⁻¹]

r_{MA} – macroalgae total respiration rate [day⁻¹]

ex_{MA} – macroalgae excretion rate [day⁻¹]

m_{MA} – macroalgae natural mortality rate (non-predatory) day⁻¹]

G_{MA} – grazing rate on macroalgae [day⁻¹]

MAGRAZCONS

$$\mu_{MA} = \mu_{\max}^{MA}(T_{ref}) \cdot \Psi(T) \cdot \Psi(I) \cdot \text{Min}(\Psi(N), \Psi(P)) \quad (V.8)$$

$\mu_{\max}^{MA}(T_{ref})$ – maximum gross growth rate at the reference temperature [day⁻¹]

MAGROWTHMAX

$\Psi(T)$ – temperature limitation factor³

$\Psi(I)$ – light limitation factor

$\Psi(N)$ – nitrogen limitation factor

$\Psi(P)$ – phosphorous limitation factor

³ See section V.7

V.2.2.1 Light Limiting Factor

$$\Psi(I) = \frac{e}{k.z} \left(e^{-I_0 e^{-kz} / I_{opt}} - e^{-I_0 / I_{opt}} \right) \quad (\text{V.9})$$

h – minimum between water column height and macroalgae height [m]

I_0 – incident radiation on macroalgae [W.m^{-2}]

I_{opt} – optimum light intensity for macroalgae photosynthesis [Wm^{-2}]

k_{MA} – light extinction coefficient in the macroalgae zone [m^{-1}]

MAPHOTOIN

$$k_{MA} = \frac{a_{abs} \Phi_{MA}}{\text{Min}(h_{MA}, h_{WC})} \times \text{Max} \left(\frac{h_{MA}}{h_{WC}}, 1 \right) \quad (\text{V.10})$$

h_{MA} – macroalgae height [m]

MAHEIGHT

h_{WC} – water column height [m]

Φ_{MA} – biomass concentration [kgC.m^{-2}]

a_{abs} – carbon-specific shading area [$\text{m}^2.\text{kg}^{-1}$]

MAABSAREA

V.2.3 Nutrients Limitation Factor

$$\Psi(N) = \frac{\Phi_{NH4} + \Phi_{NO3}}{K_N^X + \Phi_{NH4} + \Phi_{NO3}} \quad (\text{V.11})$$

$$\Psi(P) = \frac{\Phi_{IP}}{K_P^X + \Phi_{IP}} \quad (\text{V.12})$$

X ≡ Phytoplankton, MacroAlgae

K_N^X – nitrogen half-saturation constant [mgN.L^{-1}]

K_P^X – phosphorus half-saturation constant [mgP.L^{-1}]

NSATCONS;
MANSATCONS
PSATCONS;
MAPSATCONS

V.2.4 Respiration

$$r_e^X = K_{re}^X e^{0.069T} \quad (\text{V.13})$$

$$r_p^X = K_{rp}^X \mu_X \quad (\text{V.14})$$

$$r_X = r_e^X + r_p^X \quad (\text{V.15})$$

X ≡ Phytoplankton, MacroAlgae

r_X – total respiration rate [day^{-1}]

r_e^X – endogenous (or dark or basal) respiration rate [day^{-1}]

r_p^X – photorespiration respiration rate [day^{-1}]

K_{re}^X – endogenous respiration constant [day^{-1}]

FENDREPC;
MAENDRESP

K_{rp}^X – fraction of actual photosynthesis which is oxidised by photorespiration [adim]

PHOTORES;
MAPHOTORES

V.2.5 Excretion

$$ex_X = K_e^X \cdot \mu_X \cdot (1 - \Psi(I)) \quad (\text{V.16})$$

X ≡ Phytoplankton, MacroAlgae

K_e^X – excretion constant [adim]

EXCRCONS;
MAEXCRCONS

V.2.6 Natural Mortality

$$m_X = m_{\max}^X(T_{ref}) \frac{\frac{\Phi_X}{\mu_X}}{K_m^X + \frac{\Phi_X}{\mu_X}} \quad (\text{V.17})$$

$m_{\max}^X(T_{ref})$ – maximum mortality rate at the reference temperature [day⁻¹]

K_m^X – mortality half-saturation rate

[Phytoplankton: mgC.L⁻¹day⁻¹; MacroAlgae: kgC.m⁻².day⁻¹]

FMORTMAX;
MAMORTMAX
FMORTCON;
MAMORTCONS

V.3 ZOOPLANKTON

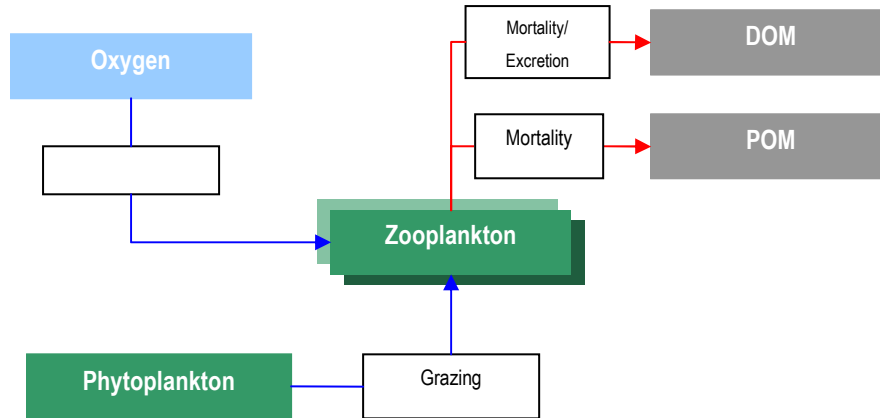


Figura V.3 – Internal flux of Zooplankton

$$\frac{\partial \Phi_{zoo}}{\partial t} = (\mu_{zoo} - r_{zoo} - m_{zoo} - p_{zoo}) \Phi_{zoo} \quad (\text{V.18})$$

μ_{zoo} – zooplankton gross growth rate [day⁻¹]

r_{zoo} – zooplankton respiration rate [day⁻¹]

m_{zoo} – zooplankton natural mortality rate [day⁻¹]

p_{zoo} – zooplankton predatory mortality rate [day⁻¹] (predation by higher trophic levels)

ZPREDMOR

$$\mu_{zoo} = \mu_{\max}^{zoo}(T_{ref}) \Psi(T) \left(1 - e^{-\Lambda (\Phi_{phy} - \Phi_{phy}^{\min})} \right) \quad (\text{V.19})$$

$\mu_{\max}^{zoo}(T_{ref})$ – zooplankton maximum gross growth rate at the reference temperature [day⁻¹]

GROWMAXZ

$\Psi(T)$ – temperature limitation factor

Λ – Ivlev grazing constant [L.mgC⁻¹]

IVLEVCON

Φ_{phy} – phytoplankton concentration [mgC.L⁻¹]

Φ_{phy}^{\min} – minimum phytoplankton concentration for the existence of grazing [mgC.L⁻¹]

GRAZFITOMIN

$$r_{zoo} + m_{zoo} = d_{zoo}(T_{ref}) \Psi(T) \quad (\text{V.20})$$

$d_{zoo}(T_{ref})$ – rate of consumption of carbon by respiration and non-predatory mortality at the reference temperature [1/day]

ZREFRESP

$\Psi(T)$ – temperature limitation factor

V.4 NITROGEN CYCLE

V.4.1 Ammonia

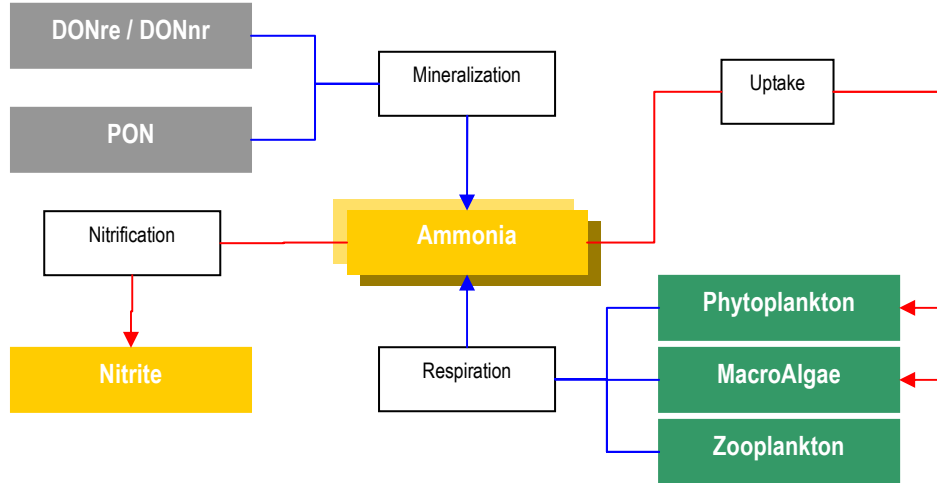


Figura V.4 – Internal flux of Ammonia

$$\begin{aligned}
 \frac{\partial \Phi_{NH4}}{\partial t} = & \underbrace{\left[f_{in/phy} (ex_{phy} + r_{phy}) \alpha_{N:C}^{phy} - \beta_{NH4}^{phy} \mu_{phy} \alpha_{N:C}^{phy} \right]}_{phytoplankton} \Phi_{phy} + \\
 & + \underbrace{\left[f_{in/MA} (ex_{MA} + r_{MA} + G_{MA}) \alpha_{N:C}^{MA} - \beta_{NH4}^{MA} \mu_{MA} \alpha_{N:C}^{MA} \right]}_{macroalgae} \frac{\Phi_{MA}}{h} \times 10^3 + \\
 & + \underbrace{\left[f_{in/zoo} (ex_{zoo} + p_{zoo}) \alpha_{N:C}^{zoo} \right]}_{zooplankton} \Phi_{zoo} + \underbrace{K_{min}^{DONre}}_{DONre} \Phi_{DONre} + \\
 & + \underbrace{f_{orgP} K_{dec}^{PON}}_{PON} \Phi_{PON} + \underbrace{K_{min}^{DONnr}}_{DONnr} \Phi_{DONnr} - \underbrace{K_{nit}}_{nitrification\ step\ 1} \Phi_{NH4}
 \end{aligned} \tag{V.21}$$

$\alpha_{N:C}^{phy}$ – phytoplankton N:C ratio (Redfield's ratio) [mgN.mgC⁻¹]

FRATIONC

$\alpha_{N:C}^{MA}$ – macroalgae N:C ratio (Atkinson's ratio) [mgN.mgC⁻¹]

MARATIONC

$\alpha_{N:C}^{bact}$ – bacteria N:C ratio [mgN.mgC⁻¹]

BRATIONC

$\alpha_{N:C}^{cil}$ – microzooplankton N:C ratio [mgN.mgC⁻¹]

CRATIONC

$\alpha_{N:C}^{zoo}$ – zooplankton N:C ratio [mgN.mgC⁻¹]

ZRATIONC

$f_{in/phy}$ – soluble inorganic fraction of the phytoplankton excretions⁴ [adim]

FSOLEXCR

$f_{in/MA}$ – soluble inorganic fraction of the macroalgae excretions [adim]

MAINEXCR

$f_{in/zoo}$ – soluble inorganic fraction of the zooplankton excretions¹ [adim]

ZSOLEXCR

⁴ See section V.8

f_{orgP} – available PON for transformation into ammonia [adim]

PHDECOMP

h – deep layer height [m]

β_{NH4}^{phy} – phytoplankton ammonia preference factor [adim]

K_{dec}^{PON} – particulate organic nitrogen decomposition rate [day⁻¹]

K_{min}^{DONre} – refractory dissolved organic nitrogen mineralization rate [day⁻¹]

K_{nit} – nitrification rate [day⁻¹]

$$\beta_{NH4}^X = \left(\frac{\Phi_{NH4}}{K_N^X + \Phi_{NH4}} \right) \left(\frac{\Phi_{NO3}}{K_N^X + \Phi_{NO3}} \right) + \left(\frac{\Phi_{NH4}}{\Phi_{NO3} + \Phi_{NH4}} \right) \left(\frac{K_N^X}{K_N^X + \Phi_{NO3}} \right) \quad (V.22)$$

X = phytoplankton or macroalgae

$$K_{dec}^{PON} = K_{dec}^{PON}(T_{ref}) \cdot \theta_{dec}^{(T-T_{ref})} \quad (V.23)$$

$K_{dec}^{PON}(T_{ref})$ – PON reference decomposition rate [day⁻¹]

NOPREF

θ_{dec} – PON decomposition temperature coefficient [adim]

NOPCOEF

T_{ref} – reference temperature = 20°C

$$K_{min}^{DONre} = K_{min}^{DONre}(T_{ref}) \cdot \theta_{min}^{DONre(T-T_{ref})} \frac{\Phi_{phy}}{K_r^{phy} + \Phi_{phy}} \quad (V.24)$$

$K_{min}^{DONre}(T_{ref})$ – DONre mineralization rate at the reference temperature [day⁻¹]

NMINR

θ_{min}^{DONre} – DONre mineralization temperature coefficient [adim]

TMINR

K_r^{phy} – phytoplankton nutrient regeneration half-saturation constant [mgC.L⁻¹]

FREGSATC

T_{ref} – reference temperature = 20°C

$$K_{nit} = K_{nit}^{ref}(T_{ref}) \theta_{nit}^{(T-T_{ref})} \frac{\Phi_O}{K_{nit}^{sat} + \Phi_O} \quad (V.25)$$

$K_{nit}^{ref}(T_{ref})$ – nitrification rate at the reference temperature [day⁻¹]

NITRIFREF

θ_{nit} – nitrification temperature coefficient [adim]

TNITCOEF

K_{nit}^{sat} – nitrification half-saturation constant [mgO₂.L⁻¹]

NITSATCO

T_{ref} – reference temperature = 20°C

K_{min}^{DONnr} – non-refractory dissolved organic nitrogen mineralization rate [day⁻¹]

$$K_{min}^{DONnr} = K_{min}^{DONnr}(T_{ref}) \cdot \theta_{min}^{DONnr(T-T_{ref})} \frac{\Phi_{phy}}{K_r^{phy} + \Phi_{phy}} \quad (V.26)$$

$K_{min}^{DONnr}(T_{ref})$ – DONnr mineralization rate at the reference temperature [day⁻¹]

NMINENR

θ_{min}^{DONnr} – DONnr mineralization temperature coefficient [adim]

TMINNR

K_r^{phy} – phytoplankton nutrient regeneration half-saturation constant [mgC.L⁻¹]

FREGSATC

T_{ref} – reference temperature = 20°C

V.4.2 Nitrite

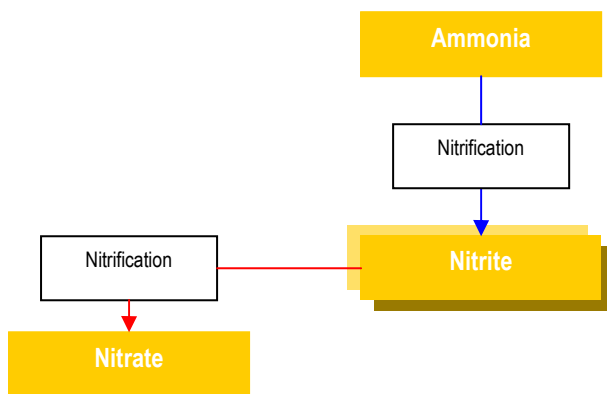


Figura V.5 – Internal flux of Nitrite

$$\frac{\partial \Phi_{NO2}}{\partial t} = K_{nit} \Phi_{NH4} - K_{nit} \Phi_{NO2} \quad (V.27)$$

V.4.3 Nitrate

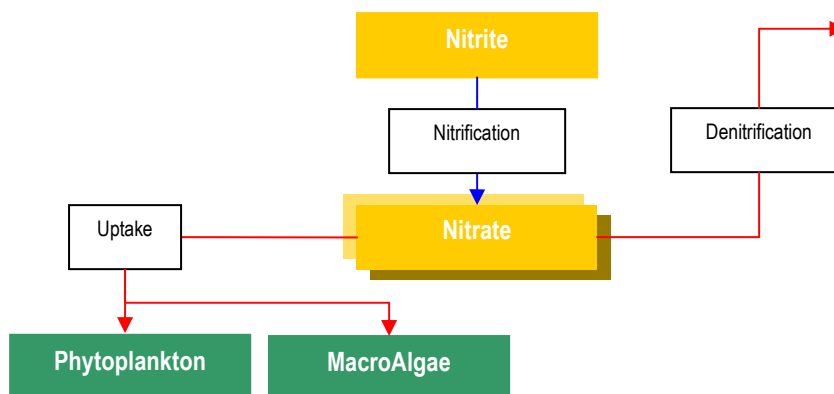


Figura V.6 – Internal flux of Nitrate

$$\frac{\partial \Phi_{NO_3}}{\partial t} = - \underbrace{(1 - \beta_{NH_4}^{phy}) \alpha_{N:C}^{phy} \mu_{phy} \Phi_{phy}}_{phytoplankton} - \underbrace{(1 - \beta_{NH_4}^{MA}) \alpha_{N:C}^{MA} \mu_{MA} \frac{\Phi_{MA}}{h} \times 10^3}_{macroalgae} + K_{nit} \Phi_{NO_2} - K_{dnit} \Phi_{NO_3} \quad (V.28)$$

$$K_{dnit} = K_{dnit}^{ref}(T_{ref}) \theta_{dnit}^{(T-T_{ref})} \frac{K_{dnit}^{sat}}{K_{dnit}^{sat} + \Phi_O} \quad (V.29)$$

$K_{dnit}^{ref}(T_{ref})$ – denitrification rate at the reference temperature [day⁻¹]

DENITREF

θ_{dnit} – denitrification temperature coefficient

TENCOEF

K_{dnit}^{sat} – denitrification half-saturation constant [mgO₂.L⁻¹]

DENSATCO

T_{ref} – reference temperature = 20°C

V.4.4 Particulate Organic Nitrogen

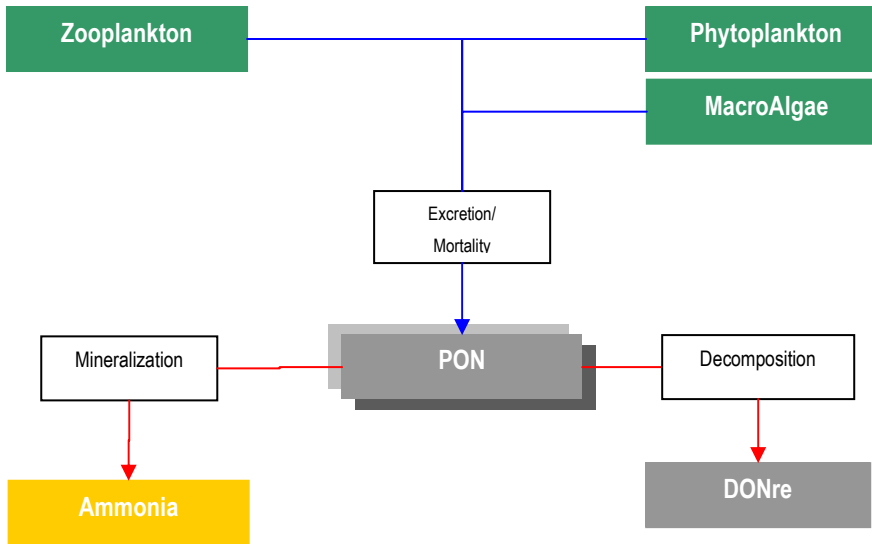


Figura V.7 – Internal flux of Particulate Organic Nitrogen

$$\begin{aligned} \frac{\partial \Phi_{PON}}{\partial t} = & \underbrace{\left[(1 - f_{in/phy})(1 - f_{orgD/phy})(ex_{phy} + r_{phy}) + m_{phy} \right] \alpha_{N:C}^{phy} \Phi_{phy}}_{phytoplankton} + \\ & + \underbrace{\left[(1 - f_{in/MA})(1 - f_{orgD/MA})(ex_{MA} + r_{MA} + G_{MA}) + m_{MA} \right] \alpha_{N:C}^{MA} \frac{\Phi_{MA}}{h} \times 10^3}_{macroalgae} - \\ & + \underbrace{\left[(1 - f_{in/zoo})(1 - f_{orgD/zoo})(r_{zoo} + p_{zoo}) + m_{zoo} \right] \alpha_{N:C}^{zoo} \Phi_{zoo} + (\delta_{phy}^N + \varphi_N) \Phi_{zoo}}_{zooplankton} - \\ & - \underbrace{(1 - f_{orgP}) K_{dec}^{PON} \Phi_{PON}}_{DONre} - \underbrace{f_{orgP} K_{dec}^{PON} \Phi_{PON}}_{ammonia} \end{aligned} \quad (V.30)$$

$f_{in/phy}$ – soluble inorganic fraction of the phytoplankton excretions	FSOLEXCR
$f_{orgD/phy}$ – dissolved organic fraction of the phytoplankton organic excretions	FDISSDON
$f_{in/zoo}$ – soluble inorganic fraction of the zooplankton excretions	ZSOLEXCR
$f_{orgD/zoo}$ – dissolved organic fraction of the zooplankton organic excretions	ZDISSDON
$f_{in/MA}$ – soluble inorganic fraction of the macroalgae excretions	MAINEXCR
$f_{orgD/MA}$ – dissolved organic fraction of the macroalgae organic excretions	MADORGEXCR
φ_N – non-assimilated phytoplankton (LostChainNitrogen)	

$$\varphi_N = \mu_{zoo} (\alpha_{N:C}^{phy} - \alpha_{N:C}^{zoo}) \quad (\text{V.31})$$

δ_{phy}^N – stoichiometric food web losses (LostPhytoGrazNitrogen)

$$\delta_{phy}^N = (1 - E) \frac{\mu_{zoo}}{E} \alpha_{N:C}^{zoo} + \varphi_N \quad (\text{V.32})$$

V.4.5 Non-Refractory Dissolved Organic Nitrogen

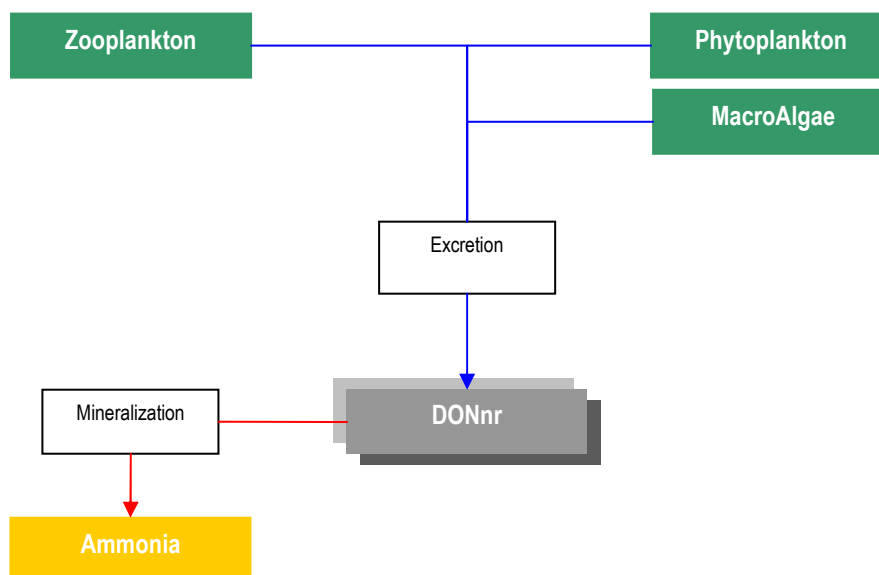


Figura V.8 – Internal flux of Non-Refractory Dissolved Organic Nitrogen

$$\begin{aligned}
\frac{\partial \Phi_{DONr}}{\partial t} = & \underbrace{(1 - f_{in/phy}) f_{orgD/phy} (ex_{phy} + r_{phy}) \alpha_{N:C}^{phy} \Phi_{phy}}_{phytoplankton} + \\
& + \underbrace{(1 - f_{in/MA}) f_{orgD/MA} (ex_{MA} + r_{MA} + G_{MA}) \alpha_{N:C}^{MA} \frac{\Phi_{MA}}{h} \times 10^3}_{macroalgae} + \\
& + \underbrace{(1 - f_{in/zoo}) f_{orgD/zoo} (ex_{zoo} + p_{zoo}) \alpha_{N:C}^{zoo} \Phi_{zoo}}_{zooplankton} - \underbrace{K_{min}^{DONr} \Phi_{DONr}}_{ammonia}
\end{aligned} \tag{V.33}$$

V.4.6 Refractory Dissolved Organic Nitrogen

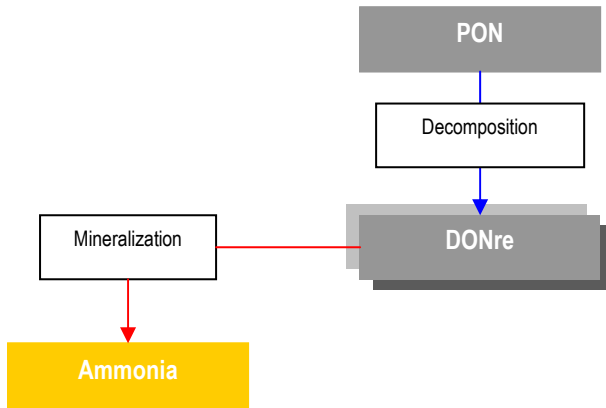


Figura V.9 – Internal flux of Refractory Dissolved Organic Nitrogen

$$\frac{\partial \Phi_{DONre}}{\partial t} = \underbrace{(1 - f_{orgP}) K_{dec}^{PON} \Phi_{PON}}_{PON} - \underbrace{K_{min}^{DONre} \Phi_{DONre}}_{ammonia} \tag{V.34}$$

V.5 PHOSPHOROUS CYCLE

V.5.1 Inorganic Phosphorus

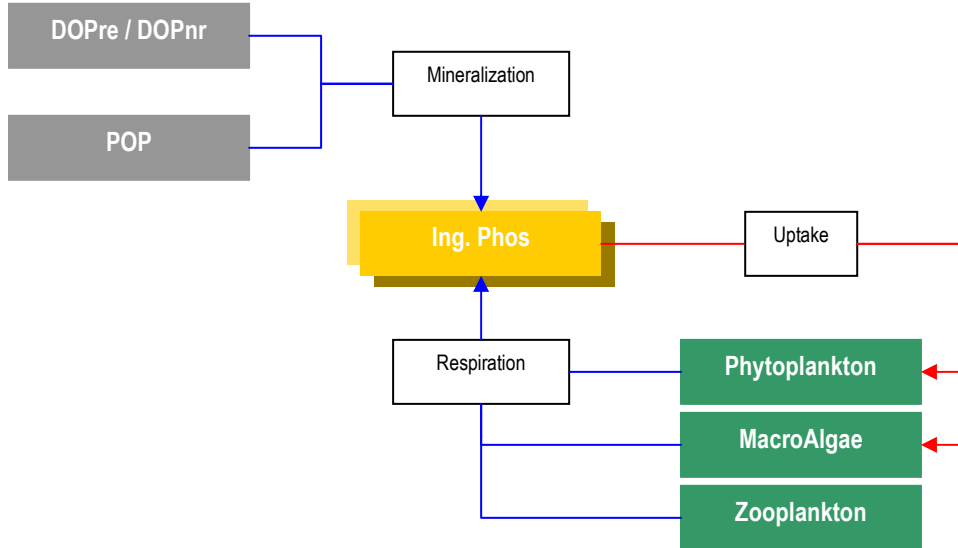


Figura V.10 – Internal flux of Inorganic Phosphorus

$$\begin{aligned}
 \frac{\partial \Phi_{IP}}{\partial t} = & \underbrace{-\mu_{phy} \alpha_{P:C}^{phy} \Phi_{phy}}_{phytoplankton} + \\
 & + \underbrace{\left[f_{in/MA} (ex_{MA} + r_{MA} + G_{MA}) \alpha_{P:C}^{MA} - \beta_{NH4}^{MA} \mu_{MA} \alpha_{P:C}^{MA} \right] \frac{\Phi_{MA}}{h} \times 10^3}_{macroalgae} + \\
 & + \underbrace{\left[f_{in/zoo} (ex_{zoo} + p_{zoo}) \alpha_{P:C}^{zoo} \right] \Phi_{zoo}}_{mesozooplankton} + \\
 & + \underbrace{K_{min}^{DOPre} \Phi_{DOPre}}_{DOPre} + \underbrace{f_{orgP} K_{dec}^{POP} \Phi_{POP}}_{POP} + \underbrace{K_{min}^{DOPnr} \Phi_{DOPnr}}_{DOPnr}
 \end{aligned} \tag{V.35}$$

$\alpha_{P:C}^{phy}$ – phytoplankton P:C ratio (Redfield's ratio) [mgP.mgC⁻¹]

FRATIOPC

$\alpha_{P:C}^{MA}$ – macroalgae P:C ratio [mgP.mgC⁻¹]

MARATIOPC

$\alpha_{P:C}^{zoo}$ – zooplankton P:C ratio [mgP.mgC⁻¹]

ZRATIOPC

K_{dec}^{POP} – particulate organic phosphorus decomposition rate [day⁻¹]

$K_{min}^{DOPre}(T_{ref})$ – DOPre mineralization rate [day⁻¹]

$K_{min}^{DOPnr}(T_{ref})$ – DOPnr mineralization rate [day⁻¹]

$$K_{dec}^{POP} = K_{dec}^{POP}(T_{ref}) \cdot \theta_{dec}^{(T-T_{ref})} \tag{V.36}$$

$K_{dec}^{POP}(T_{ref})$ – POP reference decomposition rate [day⁻¹]

PPARTMIN

θ_{dec} – POP decomposition temperature coefficient [adim]

TPPARTMINCOEF

T_{ref} – reference temperature = 20°C

$$K_{min}^{DOPre} = K_{min}^{DOPre}(T_{ref}) \cdot \theta_{min}^{DOPre}(T-T_{ref}) \frac{\Phi_{phy}}{K_r^{phy} + \Phi_{phy}} \quad (V.37)$$

$K_{min}^{DOPre}(T_{ref})$ – DOPre mineralization rate at the reference temperature [day⁻¹]

PMINR

θ_{min}^{DOPre} – DOPre mineralization temperature coefficient [adim]

PMINRCOEF

K_r^{phy} – phytoplankton nutrient regeneration half-saturation constant [mgC.L⁻¹]

FREGSATC

T_{ref} – reference temperature = 20°C

$$K_{min}^{DOPnr} = K_{min}^{DOPnr}(T_{ref}) \cdot \theta_{min}^{DOPnr}(T-T_{ref}) \frac{\Phi_{phy}}{K_r^{phy} + \Phi_{phy}} \quad (V.38)$$

$K_{min}^{DOPnr}(T_{ref})$ – DOPnr mineralization rate at the reference temperature [day⁻¹]

PMINNR

θ_{min}^{DOPnr} – DOPnr mineralization temperature coefficient [adim]

PMINNRCOEF

T_{ref} – reference temperature = 20°C

V.5.2 Particulate Organic Phosphorus

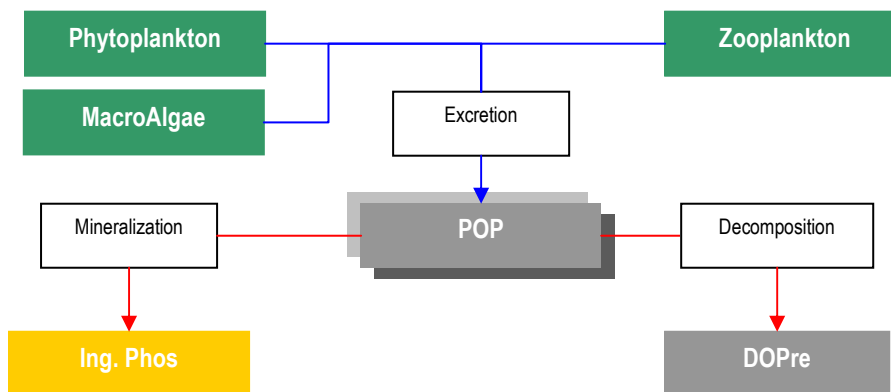


Figura V.11 – Internal flux of Particulate Organic Phosphorus

$$\begin{aligned}
\frac{\partial \Phi_{POP}}{\partial t} = & \underbrace{\left[(1 - f_{in/phy})(1 - f_{orgD/phy})(ex_{phy} + r_{phy}) + m_{phy} \right] \alpha_{P:C}^{phy} \Phi_{phy}}_{\text{phytoplankton}} + \\
& + \underbrace{\left[(1 - f_{in/MA})(1 - f_{orgD/MA})(ex_{MA} + r_{MA} + G_{MA}) + m_{MA} \right] \alpha_{P:C}^{MA} \frac{\Phi_{MA}}{h} \times 10^3}_{\text{macroalgae}} - \\
& + \underbrace{\left[(1 - f_{in/zoo})(1 - f_{orgD/zoo})(r_{zoo} + p_{zoo}) + m_{zoo} \right] \alpha_{P:C}^{zoo} \Phi_{zoo}}_{\text{zooplankton}} + (\delta_{phy}^P + \varphi_P) \Phi_{zoo} - \\
& - \underbrace{(1 - f_{orgP}) K_{dec}^{POP} \Phi_{POP}}_{DOPre} - \underbrace{f_{orgP} K_{dec}^{POP} \Phi_{POP}}_{IP}
\end{aligned} \tag{V.39}$$

φ_P – non-assimilated phytoplankton (LostChainPhosphorus)

$$\varphi_P = \mu_{zoo} (\alpha_{P:C}^{phy} - \alpha_{P:C}^{zoo}) \tag{V.40}$$

δ_{phy}^P – stoichiometric food web losses (LostPhytoGrazPhosphorus)

$$\delta_{phy}^P = (1 - E) \frac{\mu_{zoo}}{E} \alpha_{P:C}^{zoo} + \varphi_P \tag{V.41}$$

V.5.3 Non-Refractory Dissolved Organic Phosphorus

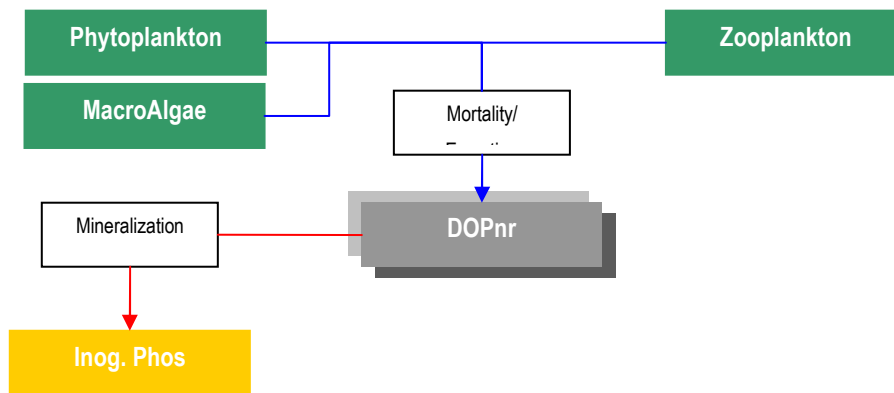


Figura V.12 – Internal flux of Non-Refractory Dissolved Organic Phosphorus

$$\begin{aligned}
\frac{\partial \Phi_{DOPnr}}{\partial t} = & \underbrace{(1 - f_{in/phy}) f_{orgD/phy} (ex_{phy} + r_{phy}) \alpha_{P:C}^{phy} \Phi_{phy}}_{\text{phytoplankton}} + \\
& + \underbrace{(1 - f_{in/MA}) f_{orgD/MA} (ex_{MA} + r_{MA} + G_{MA}) \alpha_{P:C}^{MA} \frac{\Phi_{MA}}{h} \times 10^3}_{\text{macroalgae}} - \\
& + \underbrace{(1 - f_{in/zoo}) f_{orgD/zoo} (r_{zoo} + p_{zoo}) \alpha_{P:C}^{zoo} \Phi_{zoo}}_{\text{zooplankton}} + \underbrace{K_{min}^{DOPnr} \Phi_{DOPnr}}_{IP}
\end{aligned} \tag{V.42}$$

V.5.4 Refractory Dissolved Organic Phosphorus

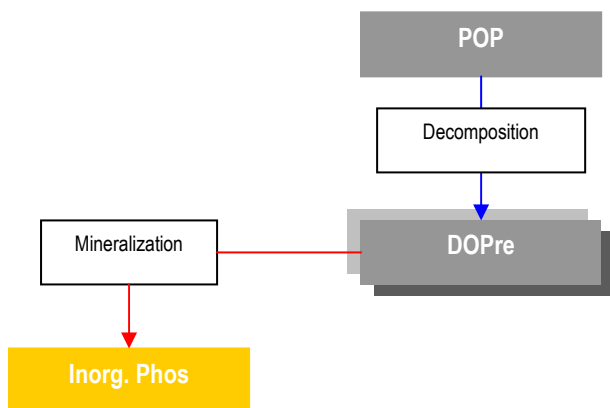


Figura V.13– Internal flux of Refractory Dissolved Organic Phosphorus

$$\frac{\partial \Phi_{DOPre}}{\partial t} = \underbrace{(1 - f_{orgP}) K_{dec}^{POP} \Phi_{POP}}_{POP} - \underbrace{K_{min}^{DOPre} \Phi_{DOPre}}_{IP} \quad (\text{V.43})$$

V.6 OXYGEN CYCLE

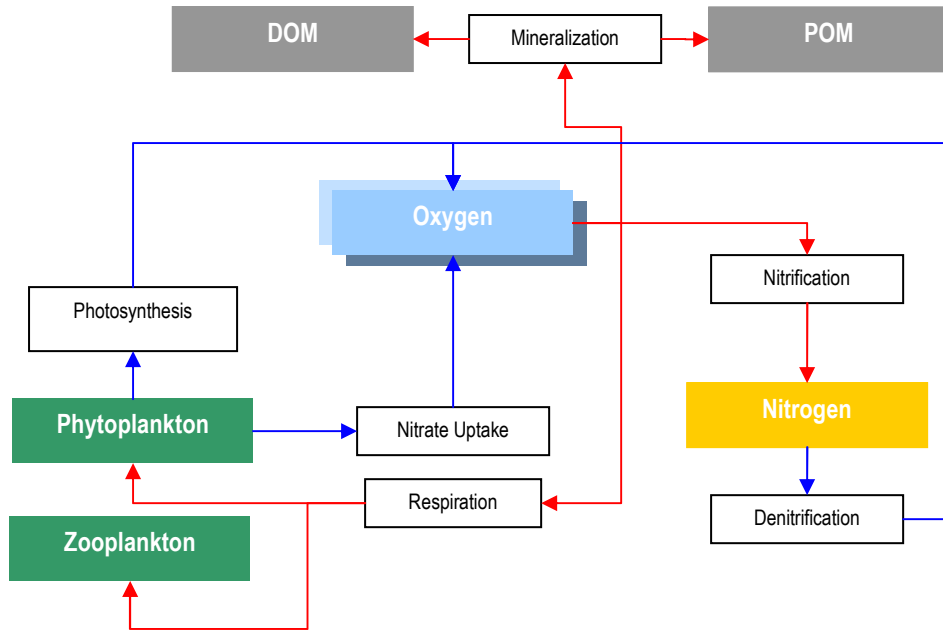


Figura V.14 - Internal Flux of Oxygen

$$\begin{aligned}
 \frac{\partial \Phi_O}{\partial t} = & \left(\underbrace{\mu_{phy} \alpha_{O:C}^{photo}}_{\text{photosynthesis}} + \underbrace{(1 - \beta_{NH4}^{phy}) \mu_{phy} \alpha_{O:N}^{NO3} \alpha_{N:C}^{phy}}_{\text{nitrate uptake}} + \underbrace{\mu_{phy} \alpha_{O:P}^{IP} \alpha_{P:C}^{phy}}_{\text{IP uptake}} - \underbrace{r_{phy} \alpha_{O:C}^{photo}}_{\text{respiration}} \right) \Phi_{phy} + \\
 & \left(\underbrace{\mu_{MA} \alpha_{O:C}^{photo}}_{\text{photosynthesis}} + \underbrace{(1 - \beta_{NH4}^{MA}) \mu_{MA} \alpha_{O:N}^{NO3} \alpha_{N:C}^{MA}}_{\text{nitrate uptake}} + \underbrace{\mu_{MA} \alpha_{O:P}^{NO3} \alpha_{P:C}^{MA}}_{\text{IP uptake}} - \underbrace{r_{MA} \alpha_{O:C}^{photo}}_{\text{respiration}} \right) \frac{\Phi_{MA}}{h} \times 10^3 + \\
 & \underbrace{(r_{zoo} + m_{zoo}) \alpha_{O:C}^{zoo} \Phi_{zoo}}_{\text{zooplankton}} - \underbrace{K_{nit}^O \Phi_{NH4}}_{\text{nitrification}} + \underbrace{K_{dnt}^O \Phi_{NO3}}_{\text{denitrification}} - \\
 & \underbrace{K_{dec}^{PON} \alpha_{min O:N} \Phi_{PON} - K_{min}^{DONre} \alpha_{min O:N} \Phi_{DONre} + K_{min}^{DONnr} \alpha_{min O:N} \Phi_{DONnr}}_{\text{organic nitrogen}} - \\
 & \underbrace{K_{dec}^{POP} \alpha_{min O:P} \Phi_{POP} - K_{min}^{DOPre} \alpha_{min O:P} \Phi_{DOPre} - K_{min}^{DOPnr} \alpha_{min O:P}^1 \Phi_{DOPnr}}_{\text{organic nitrogen}}
 \end{aligned} \tag{V.44}$$

$\alpha_{O:C}^{photo}$ – photosynthesis oxygen/carbon ratio (20/1C) = 32/12 g/g

PHOTOSOC

$\alpha_{O:C}^{plankton}$ – plankton oxygen/carbon ratio (20/1C) = 2.6 g/g

PLANK_OC_RAT

$\alpha_{O:C}^{zoo}$ – zooplankton respiration oxygen/carbon ratio (20/1C) = 32/12 g/g

ZOCRATIO

$\alpha_{O:N}^{NO_3}$ – nitrate oxygen/nitrogen ratio (3O/1N) = 48/14 g/g (secondary oxygen production due to nitrate uptake)

NITONRAT

$\alpha_{O:P}^{IP}$ – orthophosphate oxygen/phosphorus ratio (4O/1P) = 64/31 g/g (secondary oxygen production due to inorganic phosphorus uptake)

PHOSOPRAT

$$K_{nit}^O = K_{nit} \alpha_{O:N}^{nit} \Phi_O \quad (V.45)$$

$\alpha_{O:N}^{nit}$ – oxygen consumption due to nitrification ($NH_4^+ + 2O_2 \rightarrow NO_3^- + H_2O + 2H^+$) (4O/1N) [mgO/mgN] = 64/14 g/g

$$K_{dnit}^O = K_{dnit} \alpha_{O:N}^{dnit} \frac{5}{4} \quad (V.46)$$

$\alpha_{O:N}^{dnit}$ – during denitrification the organic material is decomposed, we need to convert Oxygen mass to Nitrogen mass = 32/14 mgO2/mgN

$$\alpha_{min O:N} = \frac{1}{\alpha_{N:C}^{phy}} \times \alpha_{O:C}^{CO_2} \times \frac{\Phi_O}{0.5 + \Phi_O} \quad (V.47)$$

– Mineralization oxygen/ nitrogen ratio

$$\alpha_{min O:P} = \frac{1}{\alpha_{P:C}^{phy}} \times \alpha_{O:C}^{CO_2} \times \frac{\Phi_O}{0.5 + \Phi_O} \quad (V.48)$$

– Mineralization oxygen/ phosphorus ratio

$\alpha_{min O:P}^1$ – Mineralization oxygen/ phosphorus ratio = Oxygen consumed during organic phosphorous mineralization

OPMINRATIO

$\alpha_{O:C}^{CO_2}$ – oxygen/carbon rate in CO_2 = 32/12 mgO/mgC

V.7 TEMPERATURE EFFECT

$$\Psi(T) = K_A(T) \cdot K_B(T) \quad (V.49)$$

$$K_A(T) = \frac{K_1 e^{\gamma_1(T-T_{min})}}{1 + K_1 [e^{\gamma_1(T-T_{min})} - 1]} \quad (V.50)$$

$$\gamma_1 = \frac{1}{(T_{min}^{opt} - T_{min})} \ln \left[\frac{K_2(1 - K_1)}{K_1(1 - K_2)} \right] \quad (V.51)$$

$$K_B(T) = \frac{K_4 e^{\gamma_2(T_{max} - T)}}{1 + K_4 [e^{\gamma_2(T_{max} - T)} - 1]} \quad (V.52)$$

$$\gamma_2 = \frac{1}{(T_{max} - T_{max}^{opt})} \ln \left[\frac{K_3(1 - K_4)}{K_4(1 - K_3)} \right] \quad (V.53)$$

T_{\min}^{opt} – minimum temperature for the optimal growth interval (°C)

T_{\max}^{opt} – maximum temperature for the optimal growth interval (°C)

T_{\min} – minimum tolerable temperature (°C)

T_{\max} – maximum tolerable temperature (°C)

K1, K2, K3, K4 – constants to control temperature response curve shape

TOPTFMIN; TOPTZMIN; TOPTBMIN;
MATOPTMIN

TOPTFMAX; TOPTZMAX; TOPTBMAX;
MATOPTMAX

TFMIN; TZMIN; TBMIN; MATMIN

TFMAX; TZMAX; TBMAX; MATMAX

TFCONST_i; TZCONST_i; TBCONST_i; MACONST_i

V.8 EXCRETION FRACTIONS

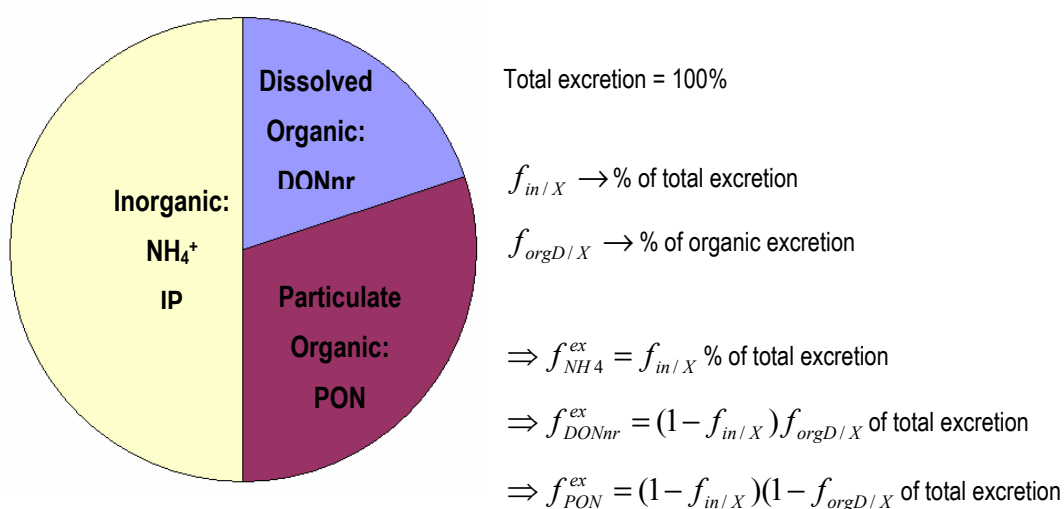


Figura V.15 – Excretion Fractions (not at scale)

APPENDIX VI

VI PARAMETERS LIST

Reference temperature = 20°C

MacroAlgae

Keyword	Variable	Description	Units	Default	Reference
MAGRAZCONS	G_{MA}	grazing rate on macroalgae	day ⁻¹	0.0008	Valiela (1995)
MAGROWTHMAX	$\mu_{\max}^{MA}(T_{ref})$	maximum gross growth rate at the reference temperature	day ⁻¹	0.4	Coffaro & Sfriso (1997); Coffaro & Bocci (1997)
MAPHOTOIN	I_{opt}	optimum light intensity for macroalgae photosynthesis	W.m ⁻²	90.0	EPA (1985)
MAHEIGHT	h_{MA}	average macroalgae bed height	m	0.2	Ferreira (1989)
MAABSAREA	a_{MA}	Carbon specific shading area	m ² kgC ⁻¹	5.55	Calibration
MANSATCONS	K_N^{MA}	nitrogen half-saturation constant	mgN.L ⁻¹	0.065	EPA (1985), Valiela (1995)
MAPSATCONS	K_P^{MA}	phosphorus half-saturation constant	mgP.L ⁻¹	0.001	EPA (1985), Valiela (1995)
MAENDRESP	K_{re}^{MA}	endogenous respiration constant	day ⁻¹	0.00175	EPA (1985), Pina (2001)
MAPHOTORES	K_{rp}^{MA}	fraction of actual photosynthesis which is oxidised by photorespiration	adim	0.018	EPA (1985), Pina (2001)
MAEXCRCONS	K_e^{MA}	excretion constant	adim	0.008	MOHID (2000)
MAMORTMAX	$m_{\max}^{MA}(T_{ref})$	maximum mortality rate at the reference temperature	day ⁻¹	0.003	Valiela (1995)
MAMORTCONS	K_m^{MA}	Macroalgae mortality half-saturation rate	kgC.m ⁻² .day ⁻¹	0.03	MOHID (2000)
MARATIONC	$\alpha_{N:C}^{MA}$	macroalgae N:C ratio (Atkinson's ratio)	mgN.mgC ⁻¹	0.064	Atkinson & Smith (1983), Baird (2001)
MARATIOPC	$\alpha_{P:C}^{MA}$	macroalgae P:C ratio	mgP.mgC ⁻¹	0.005	Atkinson & Smith (1983), Baird (2001)
MAINEXCR	$f_{in/MA}$	soluble inorganic fraction of the macroalgae excretions	adim	0.25	MOHID (2000)
MADORGEXCR	$f_{orgD/MA}$	dissolved organic fraction of the macroalgae organic excretions	adim	0.25	MOHID (2000)
MATOPTMIN	T_{\min}^{opt}	minimum temperature for the optimal growth interval	°C	12	Jones (1993)
MATOPTMAX	T_{\max}^{opt}	maximum temperature for the optimal growth interval	°C	24	Jones (1993)
MATMIN	T_{\min}	minimum tolerable temperature	°C	6	Jones (1993)
MATMAX	T_{\max}	maximum tolerable temperature	°C	37	Jones (1993)
MACONST1	K_1	constant to control temperature response curve shape	adim	0.3	MOHID (2000)
MACONST2	K_2	constant to control temperature response curve shape	adim	0.98	MOHID (2000)
MACONST3	K_3	constant to control temperature response curve shape	adim	0.98	MOHID (2000)
MACONST4	K_4	constant to control temperature response curve shape	adim	0.01	MOHID (2000)
MADEPLIM	F_{dep}^{\max}	Maximum deposition flux	gCm ⁻² s ⁻¹	0.005	Dronkers & Leussen (1988)
MAEROCRITSS	τ_{ero}^*	Detachment critical shear stress	Pa	1	Salomonsen <i>et al.</i> (1999)

Phytoplankton

Keyword	Variable	Description	Units	Default
GROWMAXF	$\mu_{\max}^{phy}(T_{ref})$	maximum gross growth rate at the reference temperature	day ⁻¹	2.2
PHOTOIN	I_{opt}	optimum light intensity for phytoplankton photosynthesis	W/m ²	100.0
NSATCONS	K_N^{Phy}	nitrogen half-saturation constant	mgN.L ⁻¹	0.014
PSATCONS	K_P^{Phy}	phosphorus half-saturation constant	mgP.L ⁻¹	0.001
FENDREPC	K_{re}^{Phy}	endogenous respiration constant	day ⁻¹	0.0175
PHOTORES	K_{rp}^{Phy}	fraction of actual photosynthesis which is oxidised by photorespiration	adim	0.018
EXCRCONS	K_e^{Phy}	excretion constant	adim	0.08
FMORTMAX	$m_{\max}^X(T_{ref})$	maximum mortality rate at the reference temperature	day ⁻¹	0.03
FMORTCON	K_m^{Phy}	phytoplankton mortality half-saturation rate	mgC.L ⁻¹ .day ⁻¹	0.3
ASS_EFIC	E	assimilation efficiency of the phytoplankton by the zooplankton	adim	0.6
FRATIONC	$\alpha_{N:C}^{phy}$	phytoplankton N:C ratio (Redfield's ratio)	mgN.mgC ⁻¹	0.18
FRATIOPC	$\alpha_{P:C}^{phy}$	phytoplankton P:C ratio (Redfield's ratio)	mgP.mgC ⁻¹	0.024
FSOLEXCR	$f_{in/phy}$	soluble inorganic fraction of the phytoplankton excretions	adim	0.4
FDISSDON	$f_{orgD/phy}$	dissolved organic fraction of the phytoplankton organic excretions	adim	0.5
TOPTFMIN	T_{min}^{opt}	minimum temperature for the optimal growth interval	°C	25.0
TOPTFMAX	T_{max}^{opt}	maximum temperature for the optimal growth interval	°C	26.5
TFMIN	T_{min}	minimum tolerable temperature	°C	4.0
TFMAX	T_{max}	maximum tolerable temperature	°C	37.0
TFCONST1	K_1	constant to control temperature response curve shape	adim	0.05
TFCONST2	K_2	constant to control temperature response curve shape	adim	0.98
TFCONST3	K_3	constant to control temperature response curve shape	adim	0.98
TFCONST4	K_4	constant to control temperature response curve shape	adim	0.02

Zooplankton

Keyword	Variable	Description	Units	Default
ZPREDMOR	P_{zoo}	zooplankton predatory mortality rate [1/day] (predation by higher trophic levels)	day ⁻¹	0.01
GROWMAXZ	$\mu_{\max}^{zoo}(T_{ref})$	zooplankton maximum gross growth rate at the reference temperature	day ⁻¹	0.1
IVLEVCON	Λ	lvlev grazing constant	L.mgC ⁻¹	13
GRAZFITOMIN	Φ_{phy}^{min}	threshold standing stock of phytoplankton below which grazing cease	mgC.L ⁻¹	0.0045
ZREFRESP	$d_{zoo}(T_{ref})$	rate of consumption of carbon by respiration and non-predatory mortality at the reference temperature	day ⁻¹	0.036
ZRATIONC	$\alpha_{N:C}^{zoo}$	Zooplankton N:C ratio	mgN.mgC ⁻¹	0.15
ZRATIOPC	$\alpha_{P:C}^{zoo}$	zooplankton P:C ratio	mgP.mgC ⁻¹	0.024
ZSOLEXCR	$f_{in/zoo}$	soluble inorganic fraction of the zooplankton excretions	adim	0.25
ZDISSDON	$f_{orgD/zoo}$	dissolved organic fraction of the zooplankton organic excretions	adim	0.25

TOPTZMIN	T_{min}^{opt}	minimum temperature for the optimal growth interval	°C	24.8
TOPTZMAX	T_{max}^{opt}	maximum temperature for the optimal growth interval	°C	25.1
TZMIN	T_{min}	minimum tolerable temperature	°C	5.0
TZMAX	T_{max}	maximum tolerable temperature	°C	35.0
TZCONST1	K_1	constant to control temperature response curve shape	adim	0.05
TZCONST2	K_2	constant to control temperature response curve shape	adim	0.98
TZCONST3	K_3	constant to control temperature response curve shape	adim	0.98
TZCONST4	K_4	constant to control temperature response curve shape	adim	0.02

Nitrogen

Keyword	Variable	Description	Units	Default
PHDECOMP	f_{orgP}	available PON for transformation into ammonia	adim	0.7
NOPREF	$K_{dec}^{PON}(T_{ref})$	PON reference decomposition rate	day ⁻¹	0.1
NMINR	$K_{min}^{DONre}(T_{ref})$	DONre mineralization rate at the reference temperature	day ⁻¹	0
NMINENR	$K_{min}^{DONnr}(T_{ref})$	DONnr mineralization rate at the reference temperature	day ⁻¹	0.1
NOPCOEF	θ_{dec}	PON decomposition temperature coefficient	adim	1.02
TMINR	θ_{min}^{DONre}	DONre mineralization temperature coefficient	adim	1.02
TMINNR	θ_{min}^{DONnr}	DONnr mineralization temperature coefficient	adim	1.02
FREGSATC	K_r^{phy}	phytoplankton nutrient regeneration half-saturation constant	mgC.L ⁻¹	1.0
NITRIFEF	$K_{nit}^{ref}(T_{ref})$	nitrification rate at the reference temperature	day ⁻¹	0.06
TNITCOEF	θ_{nit}	nitrification temperature coefficient	adim	1.08
NITSATCO	K_{nit}^{sat}	nitrification half-saturation constant	mgO ₂ .L ⁻¹	2.0
DENITREF	$K_{dnit}^{ref}(T_{ref})$	denitrification rate at the reference temperature	day ⁻¹	0.125
TDENCOEF	θ_{dnit}	denitrification temperature coefficient	aim	1.046
DENSATCO	K_{dnit}^{sat}	denitrification half-saturation constant	mgO ₂ .L ⁻¹	0.1

Phosphorus

Keyword	Variable	Description	Units	Default
PPARTMIN	$K_{dec}^{POP}(T_{ref})$	POP reference decomposition rate	day ⁻¹	0.03
TPPARTMINCOEF	θ_{dec}	POP decomposition temperature coefficient	adim	1.08
PMINR	$K_{min}^{DOPre}(T_{ref})$	DOPre mineralization rate at the reference temperature	day ⁻¹	0.0
PMINRCOEF	θ_{min}^{DOPre}	DOPre mineralization temperature coefficient	adim	1.064
PMINNR	$K_{min}^{DOPnr}(T_{ref})$	DOPnr mineralization rate at the reference temperature	day ⁻¹	0.22
PMINNRCOEF	θ_{min}^{DOPnr}	DOPnr mineralization temperature coefficient	adim	1.064

Oxygen

Keyword	Variable	Description	Units	Default
PHOTOSOC	$\alpha_{O:C}^{photo}$	photosynthesis oxygen/carbon ratio (2O/1C) = 32/12 g/g	adim	32/12
PLANK_OC_RAT	$\alpha_{O:C}^{plankton}$	plankton oxygen/carbon ratio (2O/1C) = 2.6 g/g	adim	2.6
ZOCRATIO	$\alpha_{O:C}^{zoo}$	zooplankton respiration oxygen/carbon ratio (2O/1C) = 32/12 g/g	adim	32/12
NITONRAT	$\alpha_{O:N}^{NO3}$	nitrate oxygen/nitrogen ratio (3O/1N) = 48/14 g/g (secondary oxygen production due to nitrate uptake)	adim	48/14
PHOSOPRAT	$\alpha_{O:P}^{IP}$	orthophosphate oxygen/phosphorus ratio (4O/1P) = 64/31 g/g (secondary oxygen production due to inorganic phosphorus uptake)	adim	64/31
OPMINRATIO	$\alpha_{min O:P}^1$	Mineralization oxygen/ phosphorus ratio	adim	127.27